Social Experience Shapes Fighting Strategies for Reproductive Success

Can Gao[1*], Mingze Ma[1*], Jie Chen[1], Xiaoxiao Ji[1], Qionglin Peng[1#], Yufeng Pan[1,2#]

Affiliations

[1]The Key Laboratory of Developmental Genes and Human Disease, Jiangsu Key Laboratory of Brain Science and Medicine, School of Life Science and Technology, Southeast University, Nanjing, 210096, China.

[2]Co-innovation Center of Neuroregeneration, Nantong University, Nantong, 226019, China.

[*]These authors contributed equally to this study.

[#]Correspondence to: pany@seu.edu.cn (Y.P.) or pengqionglin@seu.edu.cn (Q.P.)

Abstract

Social isolation generally increases aggression but decreases mating competition, resulting in an intricate and ambiguous relationship between social experience, aggression, and reproductive success. In male *Drosophila*, aggression is often characterized by lunging, a frequent and comparatively gentle combat behavior. Here, we provide a behavioral paradigm for studying a less frequent but more vigorous fighting form known as tussling. While social enrichment decreases lunging, aligning with past observations, it heightens the more forceful tussling behavior. These two forms of aggression rely on different olfactory receptor neurons, specifically Or67d for lunging and Or47b for tussling. We further identify three pairs of central pC1 neurons that specifically promote tussling. Moreover, shifting from lunging to tussling in socially enriched males is accompanied with better territory control and mating success. Our findings identify distinct sensory and central neurons for two fighting forms and suggest how social experience shapes fighting strategies to optimize reproductive success.

Keywords: Fighting strategies, social experience, aggression, *Drosophila melanogaster*, *Or47b* ORNs, pC1 neurons, reproductive competition

Introduction

Competition for resources such as territory, food, and mates is crucial for animal survival and reproduction (Bergman et al., 2010; Hoffmann and Cacoyianni, 1990; Stockley and Campbell, 2013; Zwarts et al., 2012). Among diverse competitive strategies, physical combat is a prevalent form of fighting to repel rivals and regulated by both genetic factors and social environment (Chen, 2022; Zwarts et al., 2012). Understanding how social experience influences combat behaviors in animals to maximize their survival and reproduction remains a fundamentally important yet inadequately understood question.

In the fruit fly, *Drosophila melanogaster*, inter-male aggression includes relative low-intensity fights such as lunging, in which one fly rears up on its hind legs and snaps down onto its opponent, as well as relative high-intensity fights like tussling, where two males tumble over each other (Certel and Kravitz, 2012; Chen et al., 2002; Hoopfer, 2016; Palavicino-Maggio and Sengupta, 2022). A recent work showed that lunges are insufficient to establish dominance but mainly serves to maintain social status, while tussling frequence is correlated with dominance establishment (Simon and Heberlein, 2020). It is noteworthy that the majority of studies focus on the low-intensity lunging behavior, owing to its higher frequency and ease of observation. Substantial studies have identified regulatory genes and the neural circuit underlying the lunging-based aggressive behaviors (Hoopfer, 2016; Kravitz and Fernandez, 2015). In particular, the male-specific volatile pheromone 11-*cis*-vaccenyl acetate (cVA) acutely promotes lunging behavior via its olfactory receptor Or67d (Wang and Anderson, 2010). Interestingly, chronic cVA exposure in socially-enriched males reduces the level of lunging via another olfactory receptor Or65a (Liu et al., 2011). Consistently, it has been found that social isolation increases lunging frequency (Palavicino-Maggio and Sengupta, 2022; Yadav et al., 2024) by altering the expression of genes such as *Cyp6a20* (Wang et al., 2008), *Drosulfakinin* (*Dsk*) (Agrawal et al., 2020), and *Tachykinin* (*Tk*) (Asahina et al., 2014). Social isolation also increases male aggression in mice (Matsumoto et al., 2005; Zelikowsky et al., 2018) and even in humans (Ferguson et al., 2005). In mice, the TK homologue Tachykinin 2 (Tac2) responds to social isolation and promotes inter-male aggressive behaviors (Zelikowsky et al., 2018). These findings contribute to the consensus that social isolation escalates aggression, whereas social enrichment mitigates it in animal models.

Meanwhile, social enrichment increases male mating success by enhancing the sensitivity of *Or47b*-expressing olfactory receptor neurons (ORNs) to fly pheromones common to both sexes (Lin et al., 2016; Sethi et al., 2019). Artificially activating *Or47b* ORNs also improves mating advantage in a competitive assay (Dweck et al., 2015). Group housing and age-dependent juvenile hormone (JH) jointly increase the expression of the male-specific proteins from *fruitless* (fru^M), which is a master gene for male courtship behaviors (Peng et al., 2021; Sato et al., 2019; Yamamoto and Koganezawa, 2013), in the *Or47b*-expressing ORNs (Hueston et al., 2016; Sethi et al.,

2019; Zhao et al., 2020). Notably, courtship levels in single-housed (SH) wild-type males are equal to (Dankert et al., 2009; Pan and Baker, 2014), in some cases, even stronger than those in group-housed (GH) males (Dankert et al., 2009). In fact, group-housing decreases excitability of the courtship-promoting P1 neurons (Inagaki et al., 2014), which express both terminal genes in the sex determination hierarchy, *fru* and *doublesex* (*dsx*). These findings raise a question on how social enrichment, which suppresses lunging-based aggression and does not increase courtship intensity, would facilitate mating competition.

Here, we modify a behavioral paradigm for studying inter-male tussling in *Drosophila* and discover that this infrequent yet intense form of combat is enhanced by social enrichment and is crucial for territory dominance and mating competition. This process requires olfactory receptor Or47b, but not Or67d or Or65a. We further identify three pairs of central *dsx*-expressing pC1 neurons that specifically promote tussling. Moreover, we demonstrate that socially enriched males can overcome mating disadvantages associated with aging.

Results

A Paradigm for High-intensity Aggression in *Drosophila*

While studying the lunging-based aggression in *Drosophila* using a high-throughput aggression assay based on previously aggression paradigms (Certel and Kravitz, 2012; Wu et al., 2020; Zhou et al., 2008), we occasionally observed the high-intensity boxing and tussling behavior in male flies (Chen et al., 2002; Nilsen et al., 2004), which are difficult to distinguish and hereafter simply referred to as tussling. We reasoned that the intensity, instead of the frequency, could be decisive for a combat (Simon and Heberlein, 2020). Thus, although tussling is a less frequent behavior, it could serve a vital function.

To induce a higher level of tussling for further manipulation, we first introduced a fixed live virgin female in the same behavioral chamber for assaying lunging. The female fly was immobilized in the middle of the food, with its head embedded in the food and its body exposed to enhance male competition (Figure 1A). We found that males that were group-housed for 7 days showed a significantly higher frequency of tussling behavior and reduced latency to tussle in the presence of an embedded virgin female (Figure 1B). We next compared tussling in male flies of different ages. We observed a significantly higher proportion of 14-day-old males raised in groups that showed tussling behavior during the 2-hour observation period, compared to the 7-day-old males (Figure 1B). Furthermore, 2-day-old males never displayed tussling behavior. In contrast, 14-day-old males showed lowed level of lunging behavior than 7-day-old males did (Figure 1-figure supplement 1). Previous studies have shown that, in addition to mating resources, food quality is another crucial factor affecting aggressive behaviors (Lim et al., 2014). Therefore, we next assayed tussling behavior in 14-day-old males in the presence of an embedded virgin female with different concentrations

of sucrose or yeast in the food during the behavioral test. We found that these males displayed similar levels of tussling behavior with different concentrations of sucrose in the food (Figure 1C). On the contrary, male tussling intensity increased significantly with higher yeast concentrations such that more than 70% of males displayed this high-intensity fighting behavior (Figures 1D, see Figure 1-video supplement 1). Taken together, these results provide an efficient behavioral paradigm for the high-intensity tussling behavior and indicate that older males display more tussling but less lunging than younger ones.

Social Enrichment Inhibits Low-intensity Lunging but Enhances High-intensity Tussling

Previous studies have shown that social enrichment inhibits aggressive behaviors, specifically the low-intensity lunging, in male flies (Yadav et al., 2024). Therefore, we wondered whether social enrichment might also inhibit the high-intensity tussling behavior in males. To answer this question, we compared both fighting behaviors in SH and GH 14-day-old males (Figure 2A). Lunging and tussling events from each group of representative samples were exhibited in raster plots for comparison (Figure 2B). We scored lunging behavior mainly in the first 10-min of test, due to its relatively higher occurrence, and tussling behavior during the whole 2-hour observational period since males take much longer time to initiate tussling (Figure 1D). Interestingly, we found that while SH males performed more frequent lunging behavior in 10 min than GH males did, which is consistent with previous findings, they rarely showed tussling behavior. In contrast, GH males displayed a large number of tussling events within 2 hours (Figure 2B). Statistical analysis of tussling and lunging behaviors showed that GH males exhibited reduced tussling latency and enhanced tussling frequency, in addition to increased lunging latency and decreased lunging frequency, compared to SH males (Figures 2C-F). We also quantified the duration of each tussling and lunging events, and found that the average duration of individual lunging events was less than 0.2 second, while a tussling event lasted from seconds to minutes (Figure 2G). This further suggests that tussling is a more intense form of aggressive behavior compared to lunging. These results indicate that social enrichment inhibits low-intensity lunging but promotes high-intensity tussling in male flies.

***Or47b* ORNs Mediate Social Experience-induced Tussling Behavior**

To further investigate the sensory basis underlying the opposite regulation of lunging and tussling behaviors by social experience, we tried to examine the role of cVA-sensitive neurons, as well as other fru^M-expressing ORNs, in mediating intermale aggression. Two cVA sensory neurons, *Or67d* and *Or65a* ORNs, play crucial roles in enhancing the lunging-based aggression in SH males, in which *Or67d* ORNs mediate acute cVA stimulation and promote male aggression (Wang and Anderson, 2010), while *Or65a* ORNs mediate chronic cVA stimulation and inhibit male aggression in GH males (Liu et al., 2011). In addition, the fru^M-expressing *Or47b* ORNs are sensitive

160 to a class of pheromones common to both sexes, such as palmitoleic acid (PA) (Lin et
161 al., 2016), and their sensitivity is enhanced under group rearing conditions (Sethi et al.,
162 2019). *Ir84a* ORNs, which are also *fru*^{M}-positive, are involved in the perception of
163 mixed food odors and promote male courtship behavior (Grosjean et al., 2011). We
164 silenced *Or67d*, *Or65a*, *Or47b* or *Ir84a* ORNs by expressing the inwardly rectifying
165 potassium channel Kir2.1 (Baines et al., 2001) and assayed lunging and tussling
166 behaviors in 14-day-old GH males. We found that silencing *Or47b* ORNs, but not
167 *Or67d*, *Or65a* or *Ir84a* ORNs, significantly decreased male tussling, compared to the
168 control (Figure 3A, B). In contrast, silencing *Or67d* ORNs, but not other ORNs,
169 significantly reduced male lunging (Figure 3C, D). These loss-of-function results
170 suggest that *Or47b* ORNs mediate male tussling behavior, whereas *Or67d* ORNs
171 regulate male lunging behavior.
172 To elucidate the potential role of the Or47b receptor in mediating tussling behavior,
173 we knocked down its expression in *Or47b* ORNs using RNA interference (RNAi). Our
174 results showed a significant decrease in male tussling behavior when the Or47b receptor
175 expression was reduced (Figure 3E, F), indicating that the functionality of *Or47b* ORNs
176 in tussling is dependent on the Or47b receptor. As previous studies suggested that the
177 male-specific *fru*^{M} sustains *Or47b* expression in an activity-dependent manner (Sethi et
178 al., 2019), we next expressed microRNAs targeting *fru*^{M} (*UAS-fruMi*) (Meissner et al.,
179 2016) in *Or47b* ORNs and assayed male tussling. The efficiency of *Or47b* and *fru*^{M}
180 RNAi knockdown was both validated by quantitative PCR (Figure 3-figure supplement
181 1). We observed a slight increase of tussling latency in *fru*^{M} knocked-down males,
182 although not significantly different from the control (Figure 3E, F), suggesting that
183 Or47b, rather than Fru^{M}, plays a more crucial role in mediating male tussling.
184 To further confirm that the effect of social enrichment on tussling depends on the
185 activity of *Or47b* ORNs, we artificially activated *Or47b* ORNs by expressing the
186 bacterially derived sodium channel (NaChBac) (Ren et al., 2001) in 14-day-old SH
187 males. We found that these SH males with enhanced activity of *Or47b* ORNs showed
188 a significant increase in tussling behavior compared to control SH males. Interestingly,
189 the level of tussling in these SH males with activated *Or47b* ORNs was
190 indistinguishable from that in GH males (Figure 3G, H). These gain-of-function results
191 indicate that social enrichment acts through *Or47b* ORNs to promote male tussling.
192 Using the trans-Tango technique that labels downstream neurons in a usage-dependent
193 manner (Talay et al., 2017), we found substantially more downstream signals of *Or47b*
194 ORNs in GH males than those in SH males (Figure 3-figure supplement 2), further
195 supporting the involvement of *Or47b* ORNs under social enrichment.
196
197 **Distinct Central Brain Neurons for Lunging and Tussling**
198 We next set out to identify the central neurons involved in regulating the high-intensity
199 tussling. We found that silencing the mushroom body neurons by expressing an
200 inwardly rectifying potassium channel Kir2.1 (Baines et al., 2001) driven by *R19B03-*
201 *GAL4* did not affect male tussling, suggesting that the experience-dependent tussling

behavior is not dependent on the classical learning and memory center. Surprisingly, inactivation of the previously-identified aggression-promoting $P1^a$ and TK neurons did not affect tussling behavior (Figure 4A, B). These results imply that the central circuit for tussling behavior may be distinct from the previously reported aggression circuits. As *dsx*-expressing pC1 neurons, also termed P1 if co-expressing fru^M, are crucial for sexual and aggressive behaviors in both males and females, we also silenced two subsets of pC1 neurons ($pC1^{SS1}$ and $pC1^{SS2}$), which were sexually dimorphic, and their functions were previously characterized in females but not in males (Wang et al., 2021). We found that inactivation of $pC1^{SS2}$ but not $pC1^{SS1}$ neurons significantly reduced the tussling behavior in male flies (Figure 4A, B). The cell bodies of $pC1^{SS2}$ and $P1^a$ neurons are both located in the center of posterior brain and project to overlapping but distinct parts of the lateral protocerebral complex (Figure 4C-E). These results suggest that $pC1^{SS2}$ neurons may be key central neurons regulating tussling behavior.

To further compare the function of $P1^a$ and $pC1^{SS2}$ neurons in regulating male behaviors, we performed optogenetic activation experiments on these neurons expressing *CsChrimson*. Compared to control male pairs that did not show any significant change upon red light stimulation (Figure 4F-H), optogenetic activation of $P1^a$ neurons induced acute courtship behavior as indicated by unilateral wing extension (UWE), and upon red light removal, there was a significant increase in lunging but not tussling (Figure 4I-K), consistent with previous findings. In contrast, optogenetic activation of $pC1^{SS2}$ neurons induced strong and acute tussling behavior, with more than 50% of the time during red light in tussling, and the tussling behavior ceased immediately upon removal of red light (Figure 4L, see Figure 4-video supplement 1). Activation of $pC1^{SS2}$ neurons did not significantly affect either male lunging or courtship (Figure 4M, N). These results indicate that $pC1^{SS2}$ neurons acutely promote the high-intensity tussling behavior.

Previous studies have revealed a crucial role of $P1^a$ neurons in promoting a persistent internal state that enhances male aggression (Hoopfer et al., 2015). To test whether $P1^a$ neurons can promote both lunging and tussling behaviors, we further performed thermal activation experiments. We found that activation of $P1^a$ neurons via dTrpA1 at 30˚C induced male tussling, just like activation of $pC1^{SS2}$ neurons did (Figure 4-figure supplement 1). As thermal activation but not optogenetic activation of $P1^a$ neurons induced tussling, we reasoned that vision might be a key factor for this discrepancy, since all optogenetic experiments were performed in dark or red light. Thus, we re-performed these thermal activation experiments in dark and found that activation of $pC1^{SS2}$ but not $P1^a$ neurons induced tussling, although the level of tussling by $pC1^{SS2}$-activated males was lower compared to that in light, suggesting a crucial role of vision in male tussling. These optogenetic and themogenetic activation experiments suggest that $P1^a$ neurons can promote both lunging and tussling behaviors, but their function on tussling requires visual stimulation, while $pC1^{SS2}$ neurons play a more direct role in acutely promoting male tussling.

We next used *retro*-Tango (Sorkaç et al., 2023) and *trans*-Tango (Talay et al., 2017) techniques to explore the potential upstream and downstream circuits of $P1^{a}$ and $pC1^{SS2}$ neurons, and observed substential differences in both conditions (Figure 4-figure supplement 2), suggesting largely parallel inputs and outputs for $P1^{a}$ and $pC1^{SS2}$ neurons.

Dsx^{M} Regulates the Development and Function of $pC1^{SS2}$ Neurons

To further compare the differences between $P1^{a}$ neurons and $pC1^{SS2}$ neurons, we investigated whether $P1^{a}$ and $pC1^{SS2}$ neurons express *fru* and/or *dsx* using Fru^{M} and Dsx^{M} antibodies (Chen et al., 2021; Peng et al., 2022). We found that most $P1^{a}$ neurons were *fru*-positive and *dsx*-positive, while $pC1^{SS2}$ neurons were *dsx*-positive but *fru*-negative (Figure 5A-5D). These results suggest that *dsx* instead of *fru* may play crucial roles in the development and function of $pC1^{SS2}$ neurons.

To investigate the function of *dsx* in $pC1^{SS2}$ neurons, we knocked down *dsx* via RNAi and compared the morphological and functional changes of these neurons. We found that dsx^{M} knockdown in $pC1^{SS2}$ neurons slightly increased the number of cells from 2-3 pairs to 3-4 pairs (Figures 5E-5G), and significantly lengthened the axonal projections ventrally (Figure 5H). We reasoned that these developmental abnormality may effect the tussling-promoting functions of $pC1^{SS2}$ neurons, and tried to activate these neurons with or without knocking down *dsx*. We found that males with wild-type *dsx* function displayed intensive tussling behavior for approximately 50% and 70% of the total activation time, respectively, during the first and second activation periods, with the response returning to baseline levels after the removal of red light (Figure 5I, 5K). However, males with *dsx* knocked down in $pC1^{SS2}$ neurons showed no tussling behavior during the first activation session, and few tussling behavior during the second activation session (Figure 5J, 5K). Together, these results reveal the crucial role of the *dsx* gene in the development and tussling-promoting function of $pC1^{SS2}$ neurons.

Territory and Mating Advantage in Tussling-favored Experienced Males

As our results showed that GH males and SH males were more likely to perform the low-frequency, high-intensity tussling and the high-frequency, low intensity lunging, respectively, we wondered which fighting strategy was more practical in the competition for territory and mating resources.

To address this question, we first designed an experimental paradigm for territory competition (Figure 6A). A circular territory, which is provided with food and a fixed virgin female and separated by a wall with a small door open to the outer area, was competed by two tester males, one of which was marked on their wings. We manually analyzed the first 10 winning events, each was defined as one male successfully displacing the other from the inner resource area. The winning index was calculated as the proportional difference in the number of wins between the marked male and unmarked male. In control groups such as two GH males of the same age, we observed some ‘winner takes all’ phenomenon (one male won nearly all of the 10 encounters),

but overall, the winning index was close to zero due to the randomness of marking (see methods). We further found that while GH 7-day-old males (G7) won slightly, but not significantly, more than SH 7-day-old males (S7) (Figure 6B), older G14 males had a significant advantage over the S14 males (Figure 6C and Figure 6-figure supplement 1, Table S2, see Figure 6-video supplement 1). Additionally, we observed that when G14 males were paired with S14 males, the proportion of males performing tussling behavior was not significantly different from that between two G14 males. However, the duration of each tussling event in G14 and S14 male pairs was significantly shorter than that between two G14 males (Figure 6-figure supplement 2).

Next, we conducted further investigations into the role of social experience and the two types of fighting behaviors in mating competition (Figure 6D). Two males and one virgin female were loaded into the behavioral chamber at the same time and recorded for courtship behaviors. A winner was defined as the male that first copulated with the female. We used the copulation advance index, which was calculated as the proportional difference between marked males and unmarked males in winning copulation (see methods). We found that G7 males had no significant advantage over S7 males (Figure 6E); however, G14 males displayed a significantly increased mating advantage over S14 males (Figure 6F, see Figure 6-video supplement 2). Together, these results suggest that the tussling-favored GH males are more competitive in territory control and mating compared to the lunging-favored SH males.

The above results showed that GH males were more competitive compare to SH males, especially in older males, suggesting that social experience may play a potential role in altering age-related mating competition. To test this hypothesis, we first tested mating competition between males of different ages under the same rearing conditions. The results showed that younger males, whether reared in group or isolation, had a greater mating advantage compared to older males (G7 > G14, S7 > S14, G14 > G21, S14 > S21) (Figure 6G, Table S2). These results indicate that there is generally a disadvantage in mating competition associated with aging. We next investigated whether the mating advantage induced by social experience could compensate for the mating disadvantage caused by aging. We tested pairs of males with different ages and rearing conditions (G7 vs. S14, S7 vs. G14, G14 vs. S21, S14 vs. G21) for mating competition. We found that while 14-day-old males were less competitive than 7-day-old males regardless of the rearing condition, indicative of the aging-related disadvantage, 21-day-old GH males were significantly more competitive than 14-day-old SH males (G21 > S14) (Figure 6H).

To further investigate whether the territorial control and mating competition advantage in GH males are related to their high tussling behavior, we paired males with low tussling behavior (*Or47b-GAL4/UAS-Kir2.1* and *pC1^{SS2}/UAS-Kir2.1*) with control males for territorial control and mating competition tests. We found that males with inactivated Or47b or pC1^{SS2} neurons were incompetitive for both territorial control and mating competition compared to control males (Figure 6-figure supplement 3), further

supporting a correlation between the occurrence of tussling behavior and the acquisition of territorial and mating competition advantages.

Taken together, these results indicate that long-term social enrichment in older males increases their territorial and mating competition, which can overcome their mating disadvantage associated with aging (Figure 7).

Discussion

Regulation of physiology and behavior by social experience is an important feature across animal species. Here, we found that social experience shapes the fighting strategies of male flies, in which GH males tend to reduce the low-intensity lunging and increase the high-intensity tussling, which enhances their territorial and mating competition. We further showed that the two forms of fighting are mediated by distinct sensory and central neurons. The complex implications of these findings are discussed below.

Previous studies have found that social isolation generally enhances aggression but decreases mating competition in animal models (Palavicino-Maggio and Sengupta, 2022; Sethi et al., 2019; Yadav et al., 2024), presenting a paradox between social experience, aggression and reproductive success. Our results resolved this paradox by dissecting aggressive behaviors into the well-studied, frequently observed lunging behavior and the less frequent but high-intensity tussling behavior. We improved the behavioral paradigm for studying tussling behavior and revealed that social experience oppositely regulates lunging and tussling. It is important to note that the frequency of lunging decreases while the frequency of tussling increases from 7-day-old to 14-day-old males, suggesting a shift in fighting strategy with age. Our results further suggest that social experience may enhance male mating competition by shifting their fighting strategy to the low-frequency, high-intensity tussling, which may be more effective in combat, although direct evidence is still lacking. These results are consistent with a previous study showing a correlation between the establishment of male dominance and tussling behavior, but not lunging (Simon and Heberlein, 2020). Interestingly, we found that the mating advantage gained through social enrichment can even offset the mating disadvantage associated with aging, further supporting the vital role of shifting fighting strategies in experienced, aged males. Note that a previous study found a mating advantage in 7-day-old males compared to 2-day-old males (Lin et al., 2016), which may be due to different levels of sexual maturity, but not necessatily reflect the aging effect. These results separate the function of the two fighting forms and rectify our understanding of how social experiences regulate aggression and reproductive success.

Our results revealed distinct neural circuits underlying the two forms of fighting, spanning from primary sensory neurons to central regulatory neurons. Specifically, silencing the cVA-sensing Or67d neurons reduced male lunging but not tussling, whereas inactivating Or47b neurons impaired male tussling but not lunging. Notably, Or47b neurons respond to pheromones common to both sexes, and the sensitivity of

these sensory neurons is enhanced by social enrichment (Lin et al., 2016; Peng et al., 2021; Sethi et al., 2019). Unlike the Or67d-dependent lunging, which is primarily male-induced and socially inhibited, the Or47b-dependent tussling is promoted by social enrichment with either male or female flies. Recently, it has been found that female flies increase aggression towards mating pairs or mated females, depending on Or47b and Or67d, respectively (Gaspar et al., 2022; Wan et al., 2023). These results suggest a common function of Or47b and Or67d neurons in both sexes for regulating aggression. However, whether these neurons mediate different fighting patterns in females and how they respond to social experience in females remain unknown. Nevertheless, our results on these two sensory pathways in males provide crucial evidence for dissecting their functions.

Regarding central regulatory neurons, we identified a novel class of pC1 neurons, $pC1^{SS2}$, that specifically promote male tussling. In male flies, there are ~60 pairs of *dsx*-expressing pC1 neurons, including the well-characterized $P1^{a}$ neurons that also express fru^{M} (Asahina, 2018; Jiang and Pan, 2022); however, there are only three pairs of $pC1^{SS2}$ neurons that specifically express *dsx* but not fru^{M}, and are crucial for the high-intensity tussling in males. The three pairs of $pC1^{SS2}$ neurons may have distinct function from $P1^{a}$ neurons in several ways. (1) $P1^{a}$ neurons promotes both male courtship and aggression (Hoopfer et al., 2015; Zhao et al., 2024), whereas $pC1^{SS2}$ neurons specifically promote aggression but not courtship. A recent study also identified $pC1^{SS2}$ neurons as aggression-promoting, but their roles in different fighting modes are not depicted (Hindmarsh Sten et al., 2025). That tussling-promoting $pC1^{SS2}$ neurons specifically express *dsx* but not fru^{M} is also consistent with a previous finding that *dsx*-positive pC1 neurons, rather that fru^{M}-positive pC1 neurons, are crucial for male aggression (Koganezawa et al., 2016). (2) $P1^{a}$ neurons promotes both lunging and tussling, although their function on tussling requires additional visual stimulation. In contrast, $pC1^{SS2}$ neurons specifically promote tussling, and the presence of light enhances but is not absolutely necessary for tussling. These results align with previous findings that visual stimuli amplify P1 activation and related behaviors (Hindmarsh Sten et al., 2021; Kohatsu and Yamamoto, 2015; Pan et al., 2012), and visual stimulation is important for male aggression (Duistermars et al., 2018; Ramin et al., 2014; Schretter et al., 2020). (3) Male lunging is induced after $P1^{a}$ activation; whereas male tussling is induced during $pC1^{SS2}$ activation. These results suggest that $P1^{a}$ neurons may not directly regulate aggression but instead induce a persistent state that promote aggression in general, while $pC1^{SS2}$ neurons may play a more direct role in mediating tussling. Future studies are needed to further dissect the seemingly parallel sensory and central neuronal pathways involved in lunging and tussling, and to explore how these pathways interact during social experience and aging to optimize reproductive success.

Materials and Methods

410 **Fly Stocks**
411 Flies were maintained at 22 or 25 °C in a 12 h:12 h light: dark cycle. *Canton-S* flies
412 were used as the wild-type strain and obtained from Janelia Research Campus (Pan and
413 Baker, 2014). *Or67d-GAL4* (BDSC_9998), *Or65a-GAL4* (BDSC_9993), *Or47b-GAL4*
414 (BDSC_9984), *IR84a-GAL4* (BDSC_41734), *TK-GAL4* (BDSC_51795), *R19B03-*
415 *GAL4* (BDSC_49830), *UAS-dTrpA1* (BDSC_26263), *UAS-Kir2.1* (BDSC_6595),
416 *UAS-CsChrimson* (BDSC_82181), *UAS-myrGFP* (BDSC_32198), *retro*-Tango
417 (BDSC_99661) and *trans-Tango* (BDSC_77124) flies were obtained from
418 Bloomington *Drosophila* Stock Center (BDSC). *UAS-NaChBac* (Ren et al., 2001),
419 fru^{GAL4} (Stockinger et al., 2005), $P1^{a}$*-spGAL4* (Zhang et al., 2018), $pC1^{SS1}$*-spGAL4*
420 (Wang et al., 2021), $pC1^{SS2}$*-spGAL4* (Wang et al., 2021), *UAS-*dsx^{M}*-RNAi* (Peng et al.,
421 2022) and *UAS-fruMi* (Meissner et al., 2016) were used as previously described. *UAS-*
422 *Or47b RNAi* (THU_2599) was obtained from TsingHua Fly Center. Detailed genotypes
423 of flies were listed in Table S1.
424
425 **Male aggression assay**
426 For the aggression assays presented in Figure 1, the prepared food was evenly spread
427 into the center of behavioral chambers. There was no female in the traditional paradigm
428 (Figure 1A, left) (Wu et al., 2020; Zhou et al., 2008), while a 3-5 day old virgin female
429 was gently fixed in the center of the food with its abdomen outside in the modified
430 paradigm (Figure 1A, right). We used a fixed female to restrict its position in the center
431 of food. Then two male testers were placed into the upper chambers separated from the
432 food (with or without a fixed female) by a film barrier. All testers were loaded by cold
433 anesthesia. After a 30-minute adaptation, the film was gently removed to allow the two
434 males to fall into the behavioral chamber, and the aggressive behavior was recorded for
435 2 hours. The aggression assays in Figure 1-figure supplement 1 was performed by using
436 the paradigm without female, while other data were acquired using the modified
437 paradigm with a fixed female unless otherwise stated. In some experiments, both single-
438 housed and group-housed (30-40 males per vial) males were assayed for comparison.
439 We manually analyzed lunging and tussling behaviors in this study. Lunging is
440 characterized by a male raising its forelegs and quickly striking the opponent, and each
441 lunge typically lasts less than 0.2 seconds through detailed slow-motion analysis.
442 Tussling is characterized by both males using their forelegs and bodies to tumble over
443 each other, and this behavior may last from seconds to minutes. Tussling is often mixed
444 with boxing, in which both flies rear up and strike the opponent with forelegs. Since
445 boxing is often transient and difficult to distinguish from tussling, we referred to the
446 mixed boxing and tussling behavior simply as tussling. As we manually analyze
447 tussling for 2 hours for each pair of males, it is possible that we may miss some tussling
448 events, especially those quick ones.
449 For the quantification of lunge latency and frequency in Figures 2E, 2F, 3C, 3D,
450 and Figure 1- figures supplement 1A, 1B, we manually analyzed the videos and defined
451 the lunge latency as the time point at which the first lunging event occurred between

the two male flies after the start of the recording. We then counted the number of lunge events occurring within 10 minutes after the first lunge. For the quantification of tussle latency and frequency in Figures 1B, 1C, 1D, 2C, 2D, 3A, 3B, 3E, 3F, 3G, 3H, 4A and 4D, we manually analyzed the videos and defined the tussle latency as the time point at which the first tussling event occurred between the two male flies after the start of the recording. We defined the tussle frequency (No. of tussles in 2 hr) as the total number of tussling events that occurred within two hours from the beginning of the video.

The food recipes for the male aggression assay were listed below. A mixture of 2.5% yeast, 2.5% sucrose and 1% agar dissolved in apple juice (Huiyuan Apple juice concentrate) was used for Figure 1B; a mixture of 2.5% yeast, different concentrations of sucrose (0, 2.5%, 5% or 10%) and 1% agar dissolved in apple juice was used for Figure 1C; a mixture of different concentrations of yeast (0, 2.5%, 5% or 10%), 2.5% sucrose and 1% agar dissolved in apple juice was used for Figure 1D; A mixture of 10% yeast and 1% agar dissolved in apple juice was used for other experiments.

dTrpA1-mediated activation experiments

For thermogenetic activation assay showed in Figure 4-figure supplement 1, two 5-7 days old males were loaded into the circular chamber (d=15mm) under cold anesthesia and separated with a transparent film. Before the recording start, the chamber was transferred to the recording platform at a specific temperature (22°C or 30°C) for 30 minutes adaptation. After that, the film was removed, and the behavior was recorded for 1 hour. The 10-minute video after film extraction was used for behavioral analysis.

CsChrimson-mediated optogenetic activation experiments

For optogenetic activation assay showed in Figure 4 and 5, males were raised at 25°C on standard fly food, collected after eclosion and housed in the dark for 5-7 days on food containing 0.4 mM all *trans*-Retinal (MFCD00001550, Sigma-Aldrich, St. Louis, MO). The specific light stimulation protocols are showed in the schematic (Figure 4F). In brief, Two 5-7 days old males were loaded into the circular chamber (d=10mm) under freeze anesthesia and separated with a transparent film in the dark. Then the chamber was moved on the plane light source (IR channel: 865nm, red-light channel: 630nm) for 15 mins adaptation. Before video recording, the IR light channel was switched on and adjusted to the appropriate intensty for recording. The film was removed before the recording start, with the red-light channel switched on (constant red light, 0.02 mW/mm^2) during the 2nd and 5th minutes of the experiment. The statistics for the tussling, lunging, and unilateral wing extension (UWE) are as follows. For tussling time and UWE time, we used LifesongY software (website: https://sourceforge.net/projects/lifesongy/), which is written by Dr. Chao Guo based on LifesongX (Bernstein et al., 1992), to calculate the percentage of the total time these behaviors occurred per minute. Specifically, the "tussling time (%)" refers to the percentage of time during the observation period in which tussling behavior occurred, relative to the total observation time. Similarly, "UWE time (%)" represents the

percentage of time during the observation period in which UWE occurred. For lunges, we counted the number of lunging occurrences per minute.

Territorial competition experiment

For the territorial competition experiment in Figures 6A-6C, Figure 6-figure supplement 3A, the behavioral setup was produced using a 3D printer (Bambu Lab A1), as illustrated in the schematic, with a transparent cover plate placed on the top. The preparation of food and female were the same as the above aggression paradigm. The female was fixed in the center of the food and two male testers were placed separately in the two small chambers on both sides. Before initiating the experiment, the two barriers were closed. After a 30-minute adaptation, the barriers were opened to allow the males access to the central large chamber, and were closed once the males went inside, and the territorial behavior was recorded for 2 hours. The first 10 encounters occurring after 1 hour of recording were used for statistical analysis. The winning event was defined as a male driving the other male out of the food area. To discriminate between tester males, about half of them were marked on one of their wings using a red maker pen 24 hours before the experiment. For expreiments using males with different ages and/or housing conditions, we calculated the winning index as (num. of wins by males [upper panel] – num. of wins by males [lower panel])/10 encounters * 100%. For control expreiments using males of the same age and housing condition, we calculated the winning index as (num. of wins by unmarked males – num. of wins by marked males)/10 encounters * 100%, which is roughly zero due to the randomness of marking.

Mating competition experiment

For the mating competition experiment shown in Figure 6D-6H, Figure 6-figure supplement 3B, the wings of males were marked 24 hours prior to the experiment the same as described above. During the experiment, a 3-5 days old virgin female was placed into the chamber under freeze anesthesia and covered with a transparent film. Then the unmarked males were loaded into the chamber in the same manner and also covered with a transparent film. Finally, the marked males were loaded. After 30 minutes adaptation, two films were removed to allow the three flies to interact, and the behavior was recorded for 1 hour. The chambers without successful copulation during the 1-hour period were excluded from further analysis. For each condition, we used 120 efficient chambers with 10 random chambers collectively as one sample. For expreiments using males with different ages and/or housing conditions, the copulation advance index was defined as (num. of male winners [upper panel] – num. of male winners [lower panel])/10 chambers * 100%. For control expreiments using males of the same age and housing condition, the copulation advance index was calculated as (num. of winners by unmarked males – num. of winners by marked males)/10 chambers * 100%, which is roughly zero due to the randomness of marking. The winner was defined as the male that first copulated with the female.

536 **Quantitative Real-time PCR**
537 Adult fly samples were frozen in liquid nitrogen and decapitated by vortex. The heads
538 were then separated from the bodies using metal sieves. Each sample, consisting of 40
539 frozen heads, was used for total RNA preparation using TRIzol reagent (15596026,
540 Thermo Fisher Scientific, Waltham, MA). We purified total RNA using a DNA-freeTM
541 Kit (AM1906, Thermo Fisher Scientific, Waltham, MA) and performed reverse
542 transcription using SuperScriptTM IV (18091050, Thermo Fisher Scientific, Waltham,
543 MA) to obtain cDNA used for templates. Quantitative PCR was performed on the
544 Roche LightCycler® 96 Real-Time PCR machine using AceQ qPCR SYBR Green
545 Master Mix (Q121-02, Vazyme, Nanjing). Transcript levels were analyzed by the $2^{-\Delta CT}$
546 method using *actin* as control. Each sample was run in triplicate. Each experiment
547 was repeated three times using independent sets of genetic crosses. Primers used for
548 RT-qPCR quantification were:
549 *actin* forward: 5′-GTCGCGATTTAACCGACTACCTGA-3′
550 *actin* reverse: 5′-TCTTGCTT CGAGATCCACATCTGC-3′
551 *fru*-P1 forward: 5′-GTGTGCGTACGTTTGAGTGT-3′
552 *fru*-P1 reverse: 5′-TAATCCTGTGACGTCGCCAT-3′
553 *Or47b* forward: 5′-CAAATCTCAGCCTTCTGCGG-3′
554 *Or47b* reverse: 5′-GATACTGGCACAGCAAACTCA-3′
555
556 **Tissue Dissection, Staining, and Imaging**
557 Brains were dissected in Schneider's insect medium (S2) and fixed in 4%
558 paraformaldehyde in 0.5% Triton X-100 and 0.5% bovine serum albumin in phosphate-
559 buffered saline (PAT) for 30 min at room temperature. After 4 × 10-min washes, tissues
560 were blocked in 3% normal goat serum (NGS) for 60 min, then incubated in primary
561 antibodies diluted in 3% NGS for 4 h at room temperature and 1 day at 4°C, then
562 washed in PAT, and incubated in secondary antibodies diluted in 3% NGS for 4 h at
563 room temperature and 1 day at 4°C. The tissues were then washed thoroughly in PAT
564 and mounted for imaging. Primary antibodies used in this study include mouse anti-HA
565 (BioLegend, 901501, 1:200), rabbit anti-GFP (Invitrogen, A11122, 1:1000),
566 monoclonal mouse anti-GFP (Sigma-Aldrich, G6539, 1:500), mouse anti-Bruchpilot
567 (Developmental Studies Hybridoma Bank, nc82, 1:50), rabbit anti-Dsx^M (1:500) and
568 mouse anti-Fru^M (1:2000). Secondary antibodies used include donkey anti-mouse IgG
569 conjugated to Alexa 488 (Invitrogen, A21206, 1:500), donkey anti-mouse IgG
570 conjugated to Alexa 555 (Invitrogen, A-31570, 1:500), donkey anti-rabbit IgG
571 conjugated to Alexa 488 (Invitrogen, A-21206, 1:500) and donkey anti-rabbit IgG
572 conjugated to Alexa 555 (Invitrogen, A-31572, 1:500). Samples were imaged on Zeiss
573 900 confocal microscopes using ZEN and processed with Fiji software.
574
575 **Trans-synaptic labeling by *trans*-Tango and *retro*-Tango**
576 The *trans*-Tango or *retro*-Tango ligand with GFP was expressed under the GAL4 driver.
577 Trans-synaptic signals were marked by a membrane-associated form of tdTomato

(QUAS-mtdTomato-3xHA). The anti-HA antibody (BioLegend, 901501, 1:200) was applied to characterize the postsynaptic or presynaptic signal. For Figure 3-figure supplement 2, male testers were kept at 18 °C until eclosion and subsequently single- or group-housed at the same temperature for two weeks before dissection and imaging. For Figure 4-figure supplement 2, flies were kept at 18 °C for *trans*-Tango and 25 °C for *retro*-Tango experiments.

Brain image registration

The protocol for standard brain registration is described previously (Zhou et al., 2014). Confocal images for brains containing $P1^{a}$ neurons and $pC1^{SS2}$ neurons were registered onto a standard reference brain (Zhou et al., 2014), using a Fiji graphical user interface as described previously (Ostrovsky et al., 2013).

Statistics

Experimental flies and genetic controls were tested under the same conditions, and data were collected from at least two independent experiments. Statistical analysis was performed using GraphPad Prism 9 (https://www.graphpad.com/scientific-software/prism/) as indicated in each figure legend. Data were first verified for normal distribution by the D'Agostino–Pearson normality test. For normally-distributed data, Student's *t* test was used for pairwise comparisons, and one-way ANOVA was used for comparisons among multiple groups, followed by Tukey's multiple comparisons. For data not normally-distributed, the Mann-Whitney test was used for pairwise comparisons, and the Kruskal–Wallis test was used for comparison among multiple groups, followed by Dunn's multiple comparisons. For group matched data that were normally-distributed, the Paired *t* test signed rank test was used for pairwise comparisons, and RM one-way ANOVA was used for comparison among multiple groups, followed by RM one-way ANOVA multiple comparisons. For group matched data that were not normally-distributed, the Wilcoxon matched-pairs signed rank test was used for pairwise comparisons, and the Friedman test was used for comparison among multiple groups, followed by Dunn's multiple comparisons. For qPCR experiments, the average relative expression of three independent experiments was analyzed using Mann-Whitney test. For one group compared with zero, we used one sample *t* test. The Chi-square test was used to compare male tussling percentage between two groups.

References

Agrawal, P., Kao, D., Chung, P., and Looger, L.L. (2020). The neuropeptide Drosulfakinin regulates social isolation-induced aggression in Drosophila. Journal of Experimental Biology *223*.

Asahina, K. (2018). Sex differences in Drosophila behavior: qualitative and quantitative dimorphism. Current Opinion in Physiology *6*, 35-45.

Asahina, K., Watanabe, K., Duistermars, B.J., Hoopfer, E., González, C.R., Eyjólfsdóttir, E.A., Perona, P., and Anderson, D.J. (2014). Tachykinin-expressing neurons control male-specific aggressive

620 arousal in Drosophila. Cell *156*, 221-235.
621 Baines, R.A., Uhler, J.P., Thompson, A., Sweeney, S.T., and Bate, M. (2001). Altered electrical
622 properties in Drosophila neurons developing without synaptic transmission. The Journal of
623 Neuroscience *21*, 1523-1531.
624 Bergman, M., Olofsson, M., and Wiklund, C. (2010). Contest outcome in a territorial butterfly: the
625 role of motivation. Proceedings of the Royal Society B: Biological Sciences *277*, 3027-3033.
626 Bernstein, A.S., Neumann, E.K., and Hall, J.C. (1992). Temporal analysis of tone pulses within the
627 courtship songs of two sibling Drosophila species, their interspecific hybrid, and behavioral
628 mutants of D. melanogaster (Diptera: Drosophilidae). Journal of Insect Behavior *5*, 15-36.
629 Certel, S.J., and Kravitz, E.A. (2012). Scoring and analyzing aggression in Drosophila. Cold Spring
630 Harbor Protocols *2012*, 319-325.
631 Chen, J., Jin, S., Chen, D., Cao, J., Ji, X., Peng, Q., and Pan, Y. (2021). fruitless tunes functional
632 flexibility of courtship circuitry during development. eLife *10*, e59224.
633 Chen, M., and Sokolowski, M. B. (2022). How Social Experience and Environment Impacts
634 Behavioural Plasticity in Drosophila. Fly *16*, 68-84.
635 Chen, S., Lee, A.Y., Bowens, N.M., Huber, R., and Kravitz, E.A. (2002). Fighting fruit flies: a model
636 system for the study of aggression. Proceedings of the National Academy of Sciences of the United
637 States of America *99*, 5664-5668.
638 Dankert, H., Wang, L., Hoopfer, E.D., Anderson, D.J., and Perona, P. (2009). Automated monitoring
639 and analysis of social behavior in Drosophila. Nature Methods *6*, 297-303.
640 Duistermars, B.J., Pfeiffer, B.D., Hoopfer, E.D., and Anderson, D.J. (2018). A Brain Module for
641 Scalable Control of Complex, Multi-motor Threat Displays. Neuron *100*, 1474-1490.e1474.
642 Dweck, H.K., Ebrahim, S.A., Thoma, M., Mohamed, A.A., Keesey, I.W., Trona, F., Lavista-Llanos, S.,
643 Svatos, A., Sachse, S., Knaden, M.*, et al.* (2015). Pheromones mediating copulation and attraction
644 in Drosophila. Proceedings of the National Academy of Sciences of the United States of America
645 *112*, E2829-2835.
646 Ferguson, C.J., Averill, P.M., Rhoades, H., Rocha, D., Gruber, N.P., and Gummattira, P. (2005). Social
647 isolation, impulsivity and depression as predictors of aggression in a psychiatric inpatient
648 population. Psychiatric Quarterly *76*, 123-137.
649 Gaspar, M., Dias, S., and Vasconcelos, M.L. (2022). Mating pair drives aggressive behavior in female
650 Drosophila. Current Biology *32*, 4734-4742 e4734.
651 Grosjean, Y., Rytz, R., Farine, J.P., Abuin, L., Cortot, J., Jefferis, G.S., and Benton, R. (2011). An
652 olfactory receptor for food-derived odours promotes male courtship in Drosophila. Nature *478*,
653 236-240.
654 Hindmarsh Sten, T., Li, R., Hollunder, F., Eleazer, S., and Ruta, V. (2025). Male-male interactions
655 shape mate selection in Drosophila. Cell *188*, 1486-1503.
656 Hindmarsh Sten, T., Li, R., Otopalik, A., and Ruta, V. (2021). Sexual arousal gates visual processing
657 during Drosophila courtship. Nature *595*, 549-553.
658 Hoffmann, A.A., and Cacoyianni, Z. (1990). Territoriality in Drosophila melanogaster as a
659 conditional strategy. Animal Behaviour *40*, 526-537.
660 Hoopfer, E.D. (2016). Neural control of aggression in Drosophila. Current Opinion in Neurobiology
661 *38*, 109-118.

Hoopfer, E.D., Jung, Y., Inagaki, H.K., Rubin, G.M., and Anderson, D.J. (2015). P1 interneurons promote a persistent internal state that enhances inter-male aggression in Drosophila. eLife *4*, e11346.

Hueston, C.E., Olsen, D., Li, Q., Okuwa, S., Peng, B., Wu, J., and Volkan, P.C. (2016). Chromatin Modulatory Proteins and Olfactory Receptor Signaling in the Refinement and Maintenance of Fruitless Expression in Olfactory Receptor Neurons. PLoS Biology *14*, e1002443.

Inagaki, H.K., Jung, Y., Hoopfer, E.D., Wong, A.M., Mishra, N., Lin, J.Y., Tsien, R.Y., and Anderson, D.J. (2014). Optogenetic control of Drosophila using a red-shifted channelrhodopsin reveals experience-dependent influences on courtship. Nat Methods *11*, 325-332.

Jiang, X., and Pan, Y. (2022). Neural Control of Action Selection Among Innate Behaviors. Neuroscience Bulletin *38*, 1541-1558.

Koganezawa, M., Kimura, K.-i., and Yamamoto, D. (2016). The Neural Circuitry that Functions as a Switch for Courtship versus Aggression in Drosophila Males. Current Biology *26*, 1395-1403.

Kohatsu, S., and Yamamoto, D. (2015). Visually induced initiation of Drosophila innate courtship-like following pursuit is mediated by central excitatory state. Nature Communications *6*, 6457.

Kravitz, E.A., and Fernandez, M.P. (2015). Aggression in Drosophila. Behavioral Neuroscience *129*, 549-563.

Lim, R.S., Eyjólfsdóttir, E., Shin, E., Perona, P., and Anderson, D.J. (2014). How food controls aggression in Drosophila. PLoS One *9*, e105626.

Lin, H.H., Cao, D.S., Sethi, S., Zeng, Z., Chin, J.S.R., Chakraborty, T.S., Shepherd, A.K., Nguyen, C.A., Yew, J.Y., Su, C.Y*., et al.* (2016). Hormonal Modulation of Pheromone Detection Enhances Male Courtship Success. Neuron *90*, 1272-1285.

Liu, W., Liang, X., Gong, J., Yang, Z., Zhang, Y.H., Zhang, J.X., and Rao, Y. (2011). Social regulation of aggression by pheromonal activation of Or65a olfactory neurons in Drosophila. Nature Neuroscience *14*, 896-902.

Matsumoto, K., Pinna, G., Puia, G., Guidotti, A., and Costa, E. (2005). Social isolation stress-induced aggression in mice: a model to study the pharmacology of neurosteroidogenesis. Stress *8*, 85-93.

Meissner, G.W., Luo, S.D., Dias, B.G., Texada, M.J., and Baker, B.S. (2016). Sex-specific regulation of Lgr3 in Drosophila neurons. Proceedings of the National Academy of Sciences of the United States of America *113*, E1256-1265.

Nilsen, S.P., Chan, Y.-B., Huber, R., and Kravitz, E.A. (2004). Gender-selective patterns of aggressive behavior in Drosophila melanogaster. Proceedings of the National Academy of Sciences of the United States of America *101*, 12342-12347.

Ostrovsky, A., Cachero, S., and Jefferis, G. (2013). Clonal analysis of olfaction in Drosophila: image registration. Cold Spring Harbor Protocols *2013*, 347-349.

Palavicino-Maggio, C.B., and Sengupta, S. (2022). The neuromodulatory basis of aggression: Lessons from the humble fruit fly. Frontiers in Behavioral Neuroscience *16*.

Pan, Y., and Baker, B.S. (2014). Genetic identification and separation of innate and experience-dependent courtship behaviors in Drosophila. Cell *156*, 236-248.

Pan, Y., Meissner, G.W., and Baker, B.S. (2012). Joint control of Drosophila male courtship behavior by motion cues and activation of male-specific P1 neurons. Proceedings of the National Academy of Sciences of the United States of America *109*, 10065-10070.

Peng, Q., Chen, J., and Pan, Y. (2021). From fruitless to sex: On the generation and diversification of an innate behavior. Genes Brain Behavior *20*, e12772.

Peng, Q., Chen, J., Su, X., Wang, R., Han, C., and Pan, Y. (2022). The sex determination gene doublesex is required during adulthood to maintain sexual orientation. Journal of Genetics and Genomics *49*, 165-168.

Ramin, M., Domocos, C., Slawaska-Eng, D., and Rao, Y. (2014). Aggression and social experience: genetic analysis of visual circuit activity in the control of aggressiveness in Drosophila. Molecular Brain *7*, 55.

Ren, D., Navarro, B., Xu, H., Yue, L., Shi, Q., and Clapham, D.E. (2001). A prokaryotic voltage-gated sodium channel. Science *294*, 2372-2375.

Sato, K., Goto, J., and Yamamoto, D. (2019). Sex Mysteries of the Fly Courtship Master Regulator Fruitless. Frontiers in Behavioral Neuroscience *13*, 245.

Schretter, C.E., Aso, Y., Robie, A.A., Dreher, M., Dolan, M.J., Chen, N., Ito, M., Yang, T., Parekh, R., Branson, K.M.*, et al.* (2020). Cell types and neuronal circuitry underlying female aggression in Drosophila. eLife *9*.

Sethi, S., Lin, H.H., Shepherd, A.K., Volkan, P.C., Su, C.Y., and Wang, J.W. (2019). Social Context Enhances Hormonal Modulation of Pheromone Detection in Drosophila. Current Biology *29*, 3887-3898.e3884.

Simon, J.C., and Heberlein, U. (2020). Social hierarchy is established and maintained with distinct acts of aggression in male Drosophila melanogaster. Journal of Experimental Biology *223*, jeb232439.

Sorkaç, A., Moşneanu, R.A., Crown, A.M., Savaş, D., Okoro, A.M., Memiş, E., Talay, M., and Barnea, G. (2023). retro-Tango enables versatile retrograde circuit tracing in Drosophila. eLife *12*, e85041.

Stockinger, P., Kvitsiani, D., Rotkopf, S., Tirián, L., and Dickson, B.J. (2005). Neural circuitry that governs Drosophila male courtship behavior. Cell *121*, 795-807.

Stockley, P., and Campbell, A. (2013). Female competition and aggression: interdisciplinary perspectives. Philosophical Transactions of the Royal Society B: Biological Sciences *368*, 20130073.

Talay, M., Richman, E.B., Snell, N.J., Hartmann, G.G., Fisher, J.D., Sorkaç, A., Santoyo, J.F., Chou-Freed, C., Nair, N., Johnson, M.*, et al.* (2017). Transsynaptic Mapping of Second-Order Taste Neurons in Flies by trans-Tango. Neuron *96*, 783-795.e784.

Wan, X., Shen, P., Shi, K., Li, J., Wu, F., and Zhou, C. (2023). A Neural Circuit Controlling Virgin Female Aggression Induced by Mating-related Cues in Drosophila. Neuroscience Bulletin *39*, 1396-1410.

Wang, K., Wang, F., Forknall, N., Yang, T., Patrick, C., Parekh, R., and Dickson, B.J. (2021). Neural circuit mechanisms of sexual receptivity in Drosophila females. Nature *589*, 577-581.

Wang, L., and Anderson, D.J. (2010). Identification of an aggression-promoting pheromone and its receptor neurons in Drosophila. Nature *463*, 227-231.

Wang, L., Dankert, H., Perona, P., and Anderson, D.J. (2008). A common genetic target for environmental and heritable influences on aggressiveness in Drosophila. Proceedings of the National Academy of Sciences of the United States of America *105*, 5657-5663.

Wu, F., Deng, B., Xiao, N., Wang, T., Li, Y., Wang, R., Shi, K., Luo, D.-G., Rao, Y., and Zhou, C. (2020). A neuropeptide regulates fighting behavior in Drosophila melanogaster. eLife *9*, e54229.

Yadav, R.S.P., Ansari, F., Bera, N., Kent, C., and Agrawal, P. (2024). Lessons from lonely flies: Molecular and neuronal mechanisms underlying social isolation. Neuroscience and Biobehavioral Reviews *156*, 105504.

Yamamoto, D., and Koganezawa, M. (2013). Genes and circuits of courtship behaviour in Drosophila males. Nature Reviews Neuroscience *14*, 681-692.

Zelikowsky, M., Hui, M., Karigo, T., Choe, A., Yang, B., Blanco, M.R., Beadle, K., Gradinaru, V., Deverman, B.E., and Anderson, D.J. (2018). The neuropeptide Tac2 controls a distributed brain state induced by chronic social isolation stress. Cell *173*, 1265-1279.

Zhang, W., Guo, C., Chen, D., Peng, Q., and Pan, Y. (2018). Hierarchical Control of Drosophila Sleep, Courtship, and Feeding Behaviors by Male-Specific P1 Neurons. Neuroscience Bulletin *34*, 1105-1110.

Zhao, H., Jiang, X., Ma, M., Xing, L., Ji, X., and Pan, Y. (2024). A neural pathway for social modulation of spontaneous locomotor activity (SoMo-SLA) in Drosophila. Proceedings of the National Academy of Sciences of the United States of America *121*, e2314393121.

Zhao, S., Deanhardt, B., Barlow, G.T., Schleske, P.G., Rossi, A.M., and Volkan, P.C. (2020). Chromatin-based reprogramming of a courtship regulator by concurrent pheromone perception and hormone signaling. Science Advances *6*, eaba6913.

Zhou, C., Pan, Y., Robinett, C.C., Meissner, G.W., and Baker, B.S. (2014). Central brain neurons expressing doublesex regulate female receptivity in Drosophila. Neuron *83*, 149-163.

Zhou, C., Rao, Y., and Rao, Y. (2008). A subset of octopaminergic neurons are important for Drosophila aggression. Nature Neuroscience *11*, 1059-1067.

Zwarts, L., Versteven, M., and Callaerts, P. (2012). Genetics and neurobiology of aggression in Drosophila. Fly *6*, 35-48.

Figures and figure legends

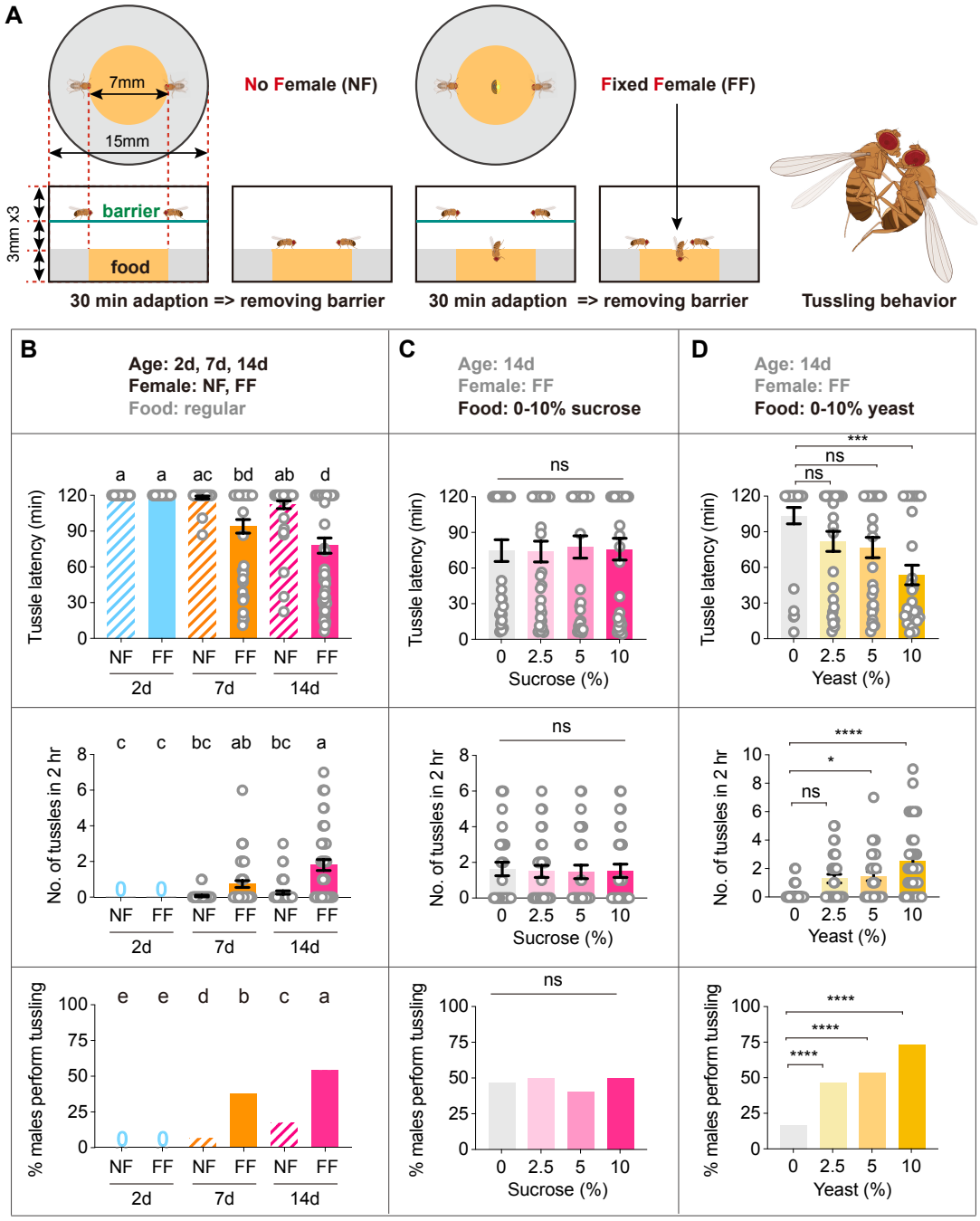

Figure 1. A paradigm for tussling behavior in male *Drosophila*.
(A) Diagrams of two fighting paradigms for *Drosophila* tussling behavior. The left diagram shows a traditional fighting paradigm with no female (NF) in the food area and a modified fighting paradigm with a fixed female (FF) in the center of the food area. Before the experiment began, two male flies were placed on the upper layer, separated from the food by a film. After a 30-minute adaptation, the film was removed to start recording. The right diagram shows a pair of tussling male *Drosophila*. All tester males in this figure were group housed.

(B) The influence of age and female factors on male tussling behavior. From top to bottom, the tussle latency, the number of tussles, and the proportion of tussles occurring are shown respectively. n=30, 30, 30, 46, 46, 46 from left to right. Bars sharing the same letter are not significantly different according to Kruskal-Wallis test (tussle latency, number of tussles) and Chi-square test (proportion of tussles occurring).
(C) Sucrose concentration of food have no effect on male tussling behavior. n=30 for each group, n.s., not significant, Kruskal-Wallis test (tussle latency, number of tussles), and Chi-square test (proportion of tussles occurring).
(D) The influence of yeast concentration on male tussling behavior. n=30 for each group, n.s., not significant, *P < 0.05, ***P < 0.001, ****P < 0.0001, Kruskal-Wallis test (tussle latency, number of tussles), and Chi-square test (proportion of tussles occurring). Error bars correspond to SEM.

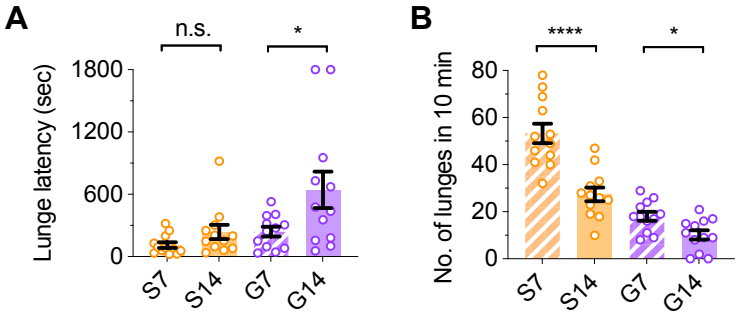

Figure 1-figure supplement 1. Aging suppresses lunging behavior in male *Drosophila*.
(A) The lunge latency in 7-day-old single-housed (S7), 14-day-old single-housed (S14), 7-day-old group-housed (G7) and 14-day-old group-housed (G14) males, n=12 for each group, n.s., not significant, *P < 0.05, Mann-Whitney test.
(B) The number of lunges in S7, S14, G7 and G14 males within 10 minutes, n=12 for each group, *P < 0.05, ****P < 0.0001, Mann-Whitney test. Error bars correspond to SEM.

Figure 1-video supplement 1. Tussling behavior between two 14-day-old group-housed (G14) wild-type males.

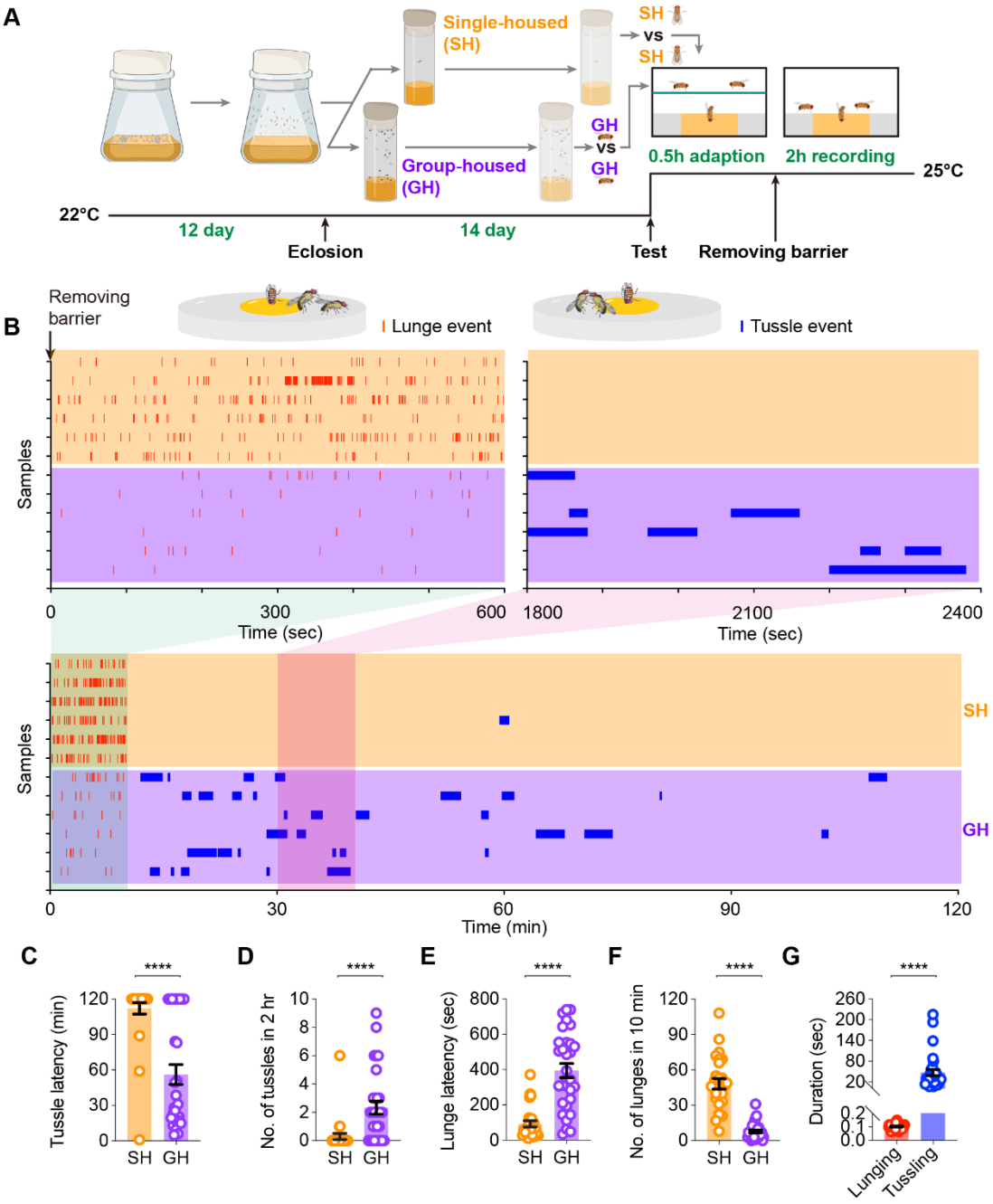

Figure 2. Social enrichment inhibits lunging behavior but promotes tussling behavior in males.

(A) Schematic diagram of *Drosophila* rearing conditions and experimental procedure.

(B) Representative raster plots illustrating lunge events in the first 10 minutes and tussle events over 2 hours in single-housed (SH) and group-housed (GH) males.

(C, D) Latency (C) and number (D) of tussling behavior in SH and GH males, n=27, 30 for SH and GH males, respectively, ****P < 0.0001, Mann-Whitney test for both.

(E, F) Latency (E) and number (F) of lunging behavior in SH and GH males, n=27, 30 for SH and GH males, respectively, ****P < 0.0001, Mann-Whitney test for both. Error bars correspond to SEM.

(G) Average duration of lunging events in the first 10 minutes and tussling events within 2 hours in GH males, n=30 events from 10 samples for each group, ****P < 0.0001, Mann-Whitney test. Error bars correspond to SEM.

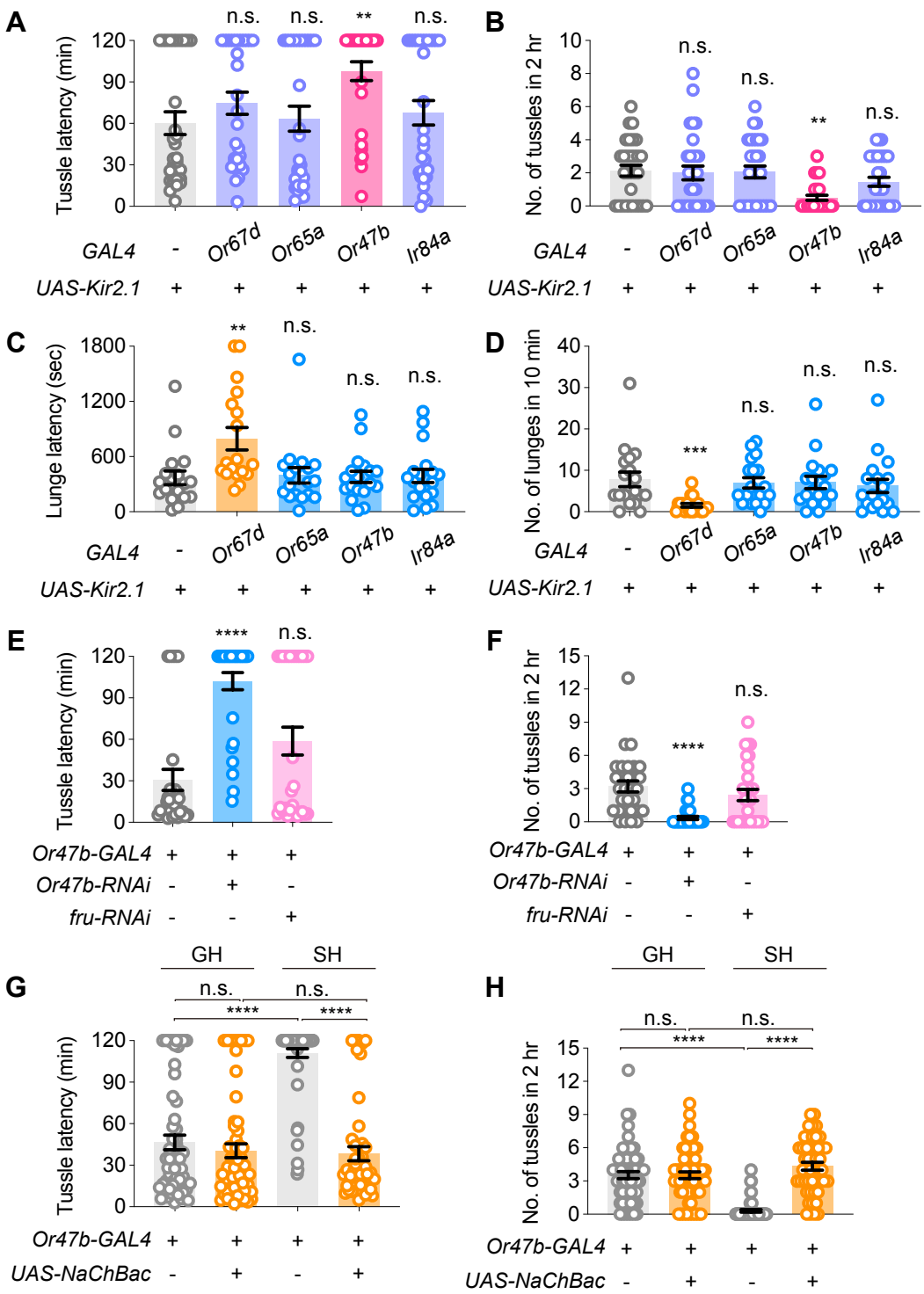

Figure 3. Or47b neurons are required for male tussling but not lunging.

825 (A, B) The effect of inactivating different sensory neurons on latency (A) and number
826 (B) of tussling behavior in 14-day-old group-housed males (G14). n=30 for each group,
827 n.s., not significant, **P < 0.01, Kruskal-Wallis test.
828 (C, D) The effect of inactivating different sensory neurons on the latency (C) and
829 number (D) of lunging behavior in G14 males. n=30 for each group, n.s., not significant,
830 **P < 0.01, ***P < 0.001, Kruskal-Wallis test.
831 (E, F) The effect of knocking down *Or47b* or *fru*^{M} expression in *Or47b* ORNs on the
832 latency (E) and number (F) of tussling behavior in G14 males, respectively. n=30 for
833 each group, n.s., not significant, ****P < 0.0001, Kruskal-Wallis test.
834 (G, H) The effect of activating *Or47b* ORNs on latency (G) and number (H) of tussling
835 behavior under conditions of GH or SH for 14 days, n=60, 60, 60, 49 respectively, n.s.,
836 not significant, ****P < 0.0001, Kruskal-Wallis test. Error bars correspond to SEM.
837

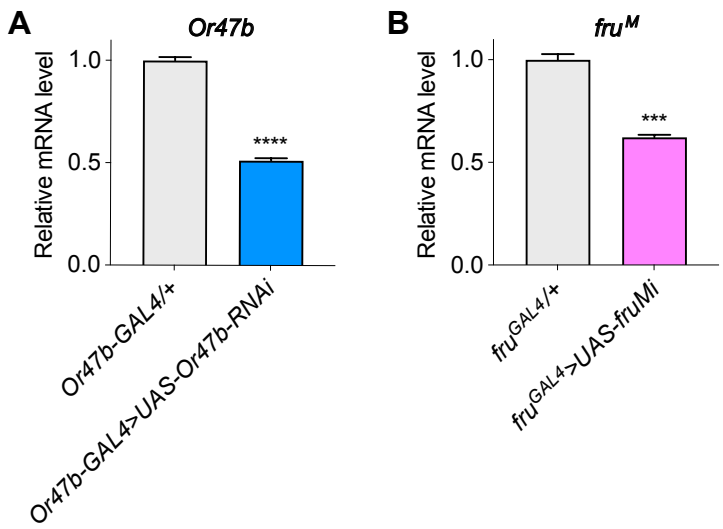

838
839 **Figure 3-figure supplement 1. Validation of the *Or47b* and *fru*^{M} RNAi efficiency**.
840 Validation of *UAS-Or47b-RNAi* (A) and *UAS-fruMi* (B) efficiency by quantitative
841 qPCR. n=9 for each of three replicates, ****P < 0.0001, ***P < 0.001, Mann-Whitney
842 test. Error bars correspond to SEM.
843

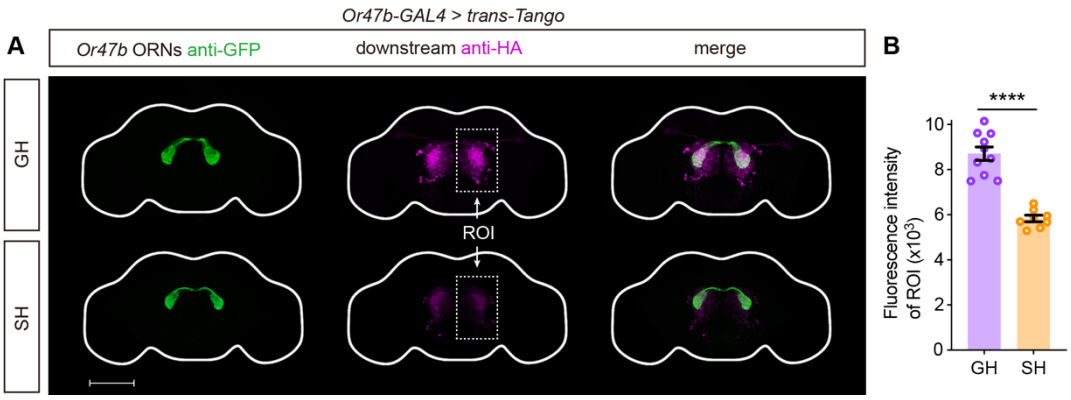

844
845 **Figure 3-figure supplement 2. Group housing increases downstream signals of**
846 ***Or47b* ORNs.**

847 (A) Projection of *Or47b* ORNs (green) and their downstream neurons (red) in GH and
848 SH conditions. Scale bar, 100μm.
849 (B) The fluorescence intensity of neurons downstream of *Or47b* ORNs is stronger
850 under GH conditions compared to SH conditions. Both groups of male testers were 14
851 days old, n=10 and 8, respectively, ****$P < 0.0001$, Mann-Whitney test. Error bars
852 correspond to SEM.
853

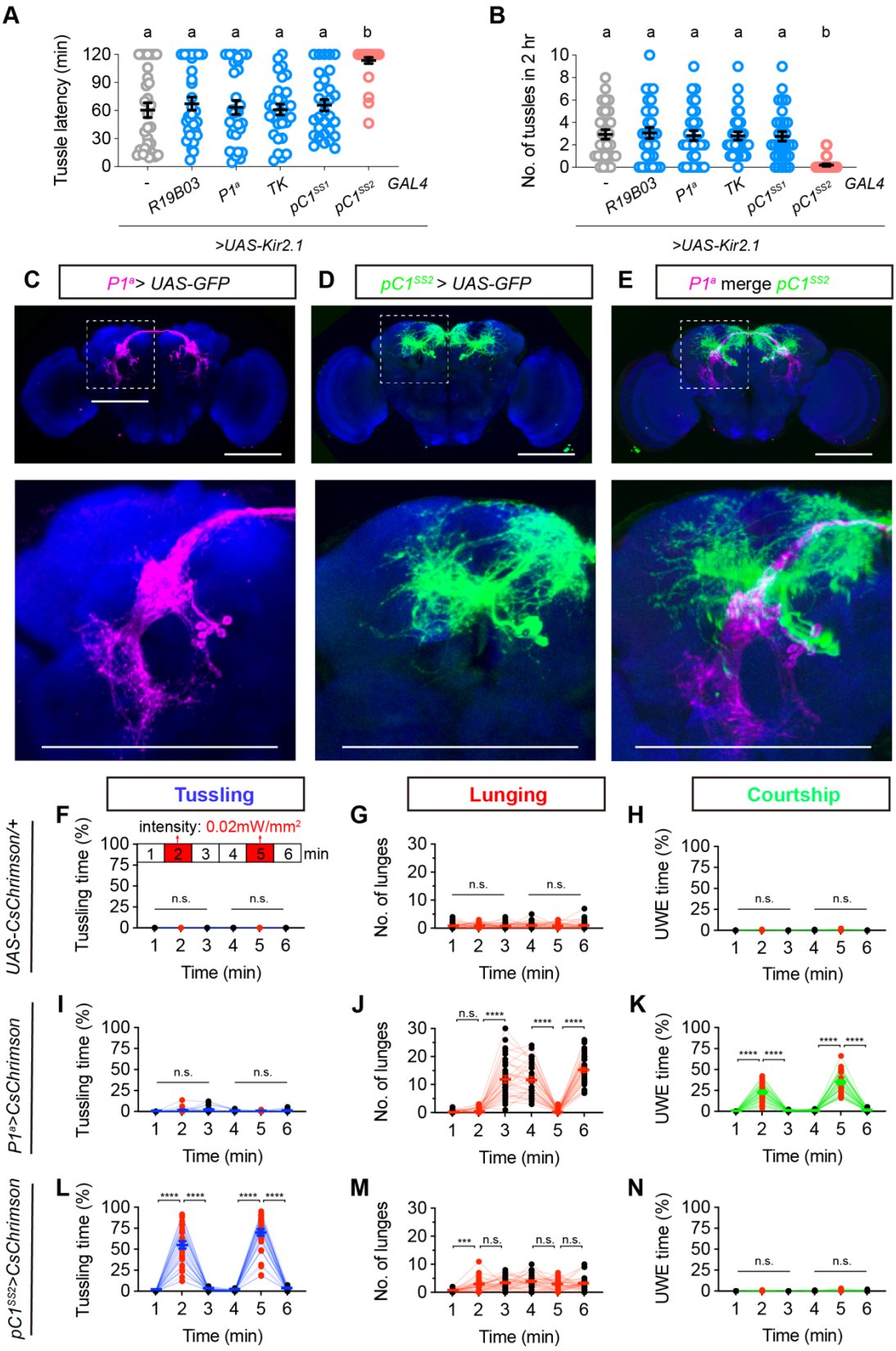

Figure 4. A subset of pC1 neurons specifically promote male tussling behavior. (A, B) The effect of inactivating candidate interneurons on latency (A) and number (B) of male tussling behavior, n=30 for each group, bars sharing the same letter are not significantly different according to Kruskal-Wallis test.

(C-E) The expression pattern of *P1^{a}-spGAL4* (C) and *pC1^{SS2}-spGAL4* (D) in male brain, and (E) the registration of P1^{a} (magenta) and pC1^{SS2} (green) neurons in a standard brain. The GFP expression indicates P1^{a} (magenta) and pC1^{SS2} (green) neurons in the male brain counterstained with nc82 (blue). White dashed boxes in (C-E) were zoomed in and shown below each panel. Scale bars, 100μm.

(F-H) Statistics on tussling (F), lunging (G) and unilateral wing extension (UWE, H) by *UAS-CsChrimson/+* males. Red light activation with a light intensity of 0.02 mW/mm^2 for 1 minute was applied at the 2nd and 5th minutes of this and subsequent experiments. n=32 for each group, n.s., not significant, Friedman test.

(I-K) Statistics on tussling (I), lunging (J) and UWE (K) in *P1^{a}>UAS-CsChrimson* males. n=32 for each group, n.s., not significant, ****P < 0.0001, Friedman test.

(L-N) Statistics on tussling (L), lunging (M) and UWE (N) in *pC1^{SS2}>UAS-CsChrimson* males. n=32 for each group, n.s., not significant, ***P < 0.001, ****P < 0.0001, Friedman test.

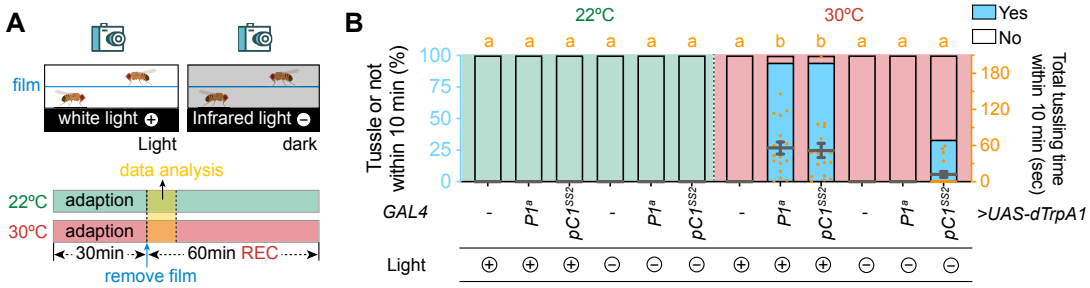

Figure 4-figure supplement 1. light-dependent initiation of male tussling behavior.

(A) Schematic diagram of the thermal activation experiment.

(B) The percentage of tussling occurrence (left) and total tussling time (right) within 10 mins. All tester males were 5 to 7-day-old group-housed males. n=18 for each group, bars sharing the same letter are not significantly different according to Kruskal-Wallis test based on the data of total tussling time.

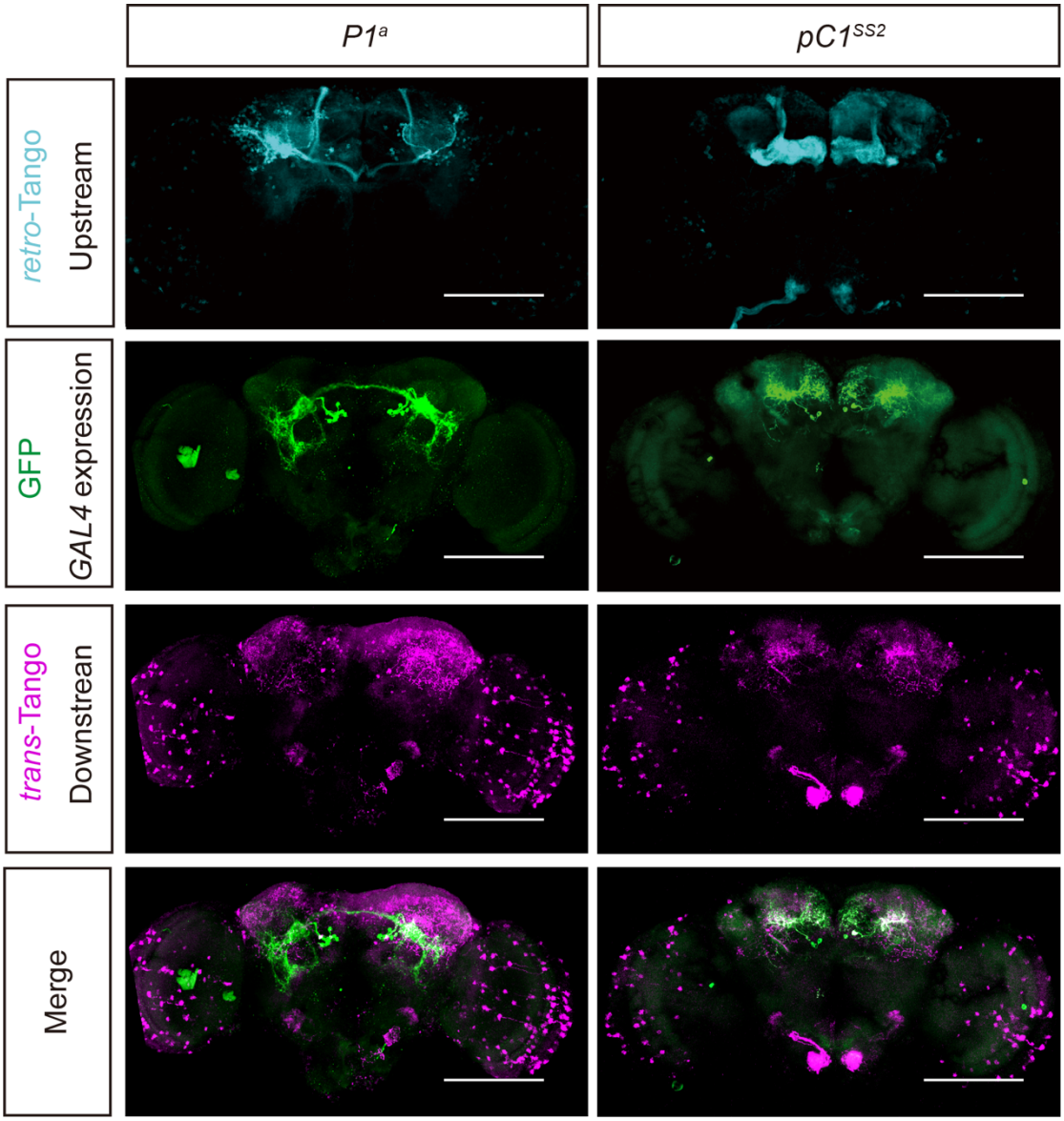

Figure 4-figure supplement 2. Immunostaining images of potential upstream signals (*retro*-Tango) and downstream signals (*trans*-Tango) of P1ᵃ and pC1^{SS2} neurons. Scale bars, 100μm.

Figure 4-video supplement 1. Optogenetic activation of pC1^{SS2} neurons acutely induces tussling in 5 to 7-day-old group-housed males (*pC1^{SS2}>UAS-CsChrimson*).

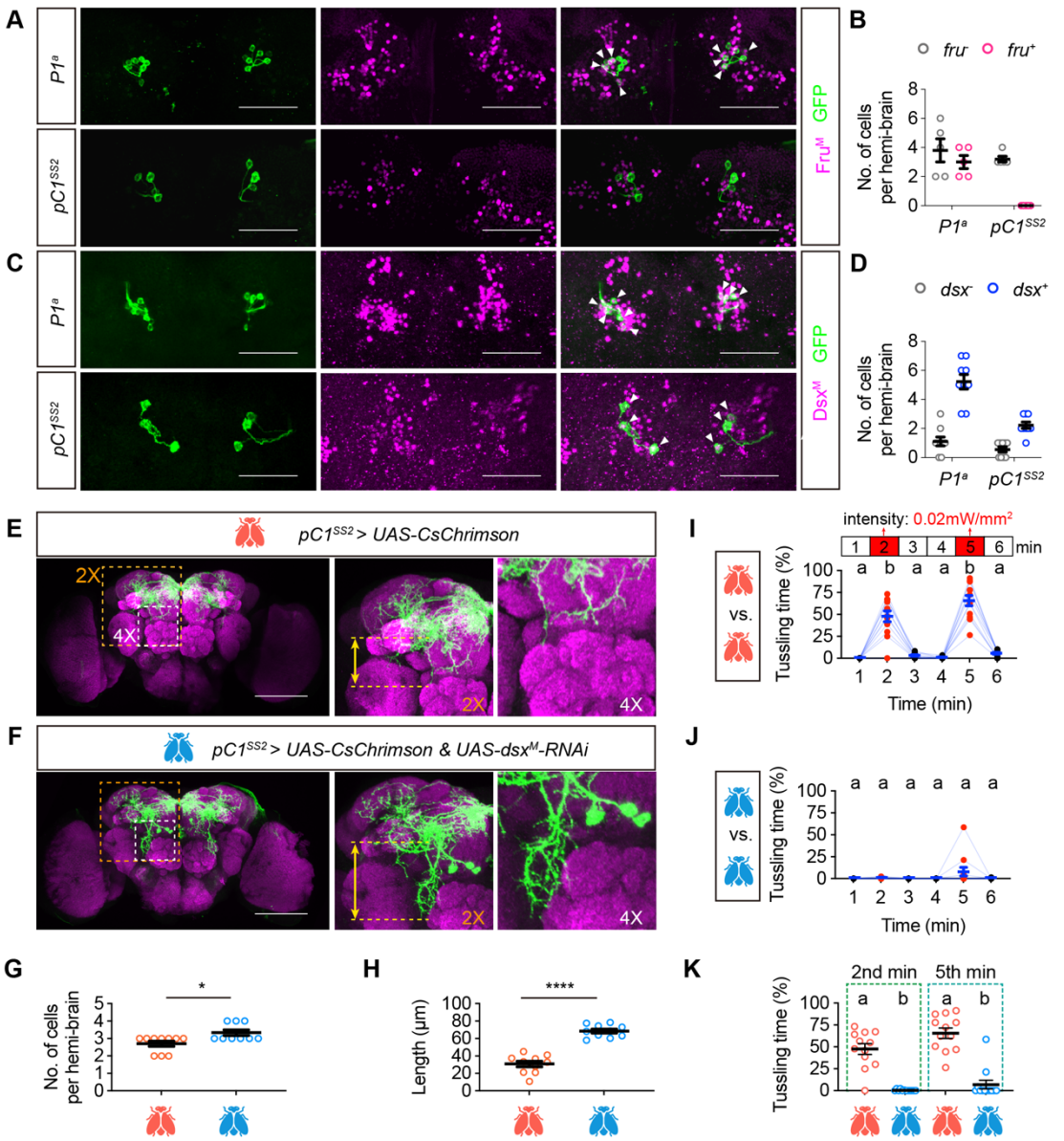

Figure 5. Dsx^{M} regulates the development and tussling-promoting function of pC1^{SS2} neurons.

(A, B) The co-staining of P1^{a} or pC1^{SS2} neurons with the Fru^{M} antibody (A), and the quantification of *fru*-positive neurons in P1^{a} and pC1^{SS2} populations (B). n=5 for each group. Scale bars, 50μm.

(C, D) The co-staining of P1^{a} or pC1^{SS2} neurons with the Dsx^{M} antibody, and The quantification of *dsx*-positive neurons in P1^{a} and pC1^{SS2} populations (D), n=9 for each group. Scale bars, 50μm.

(E-K) Knocking down *dsx* in pC1^{SS2} neurons impact their development and tussling-promoting function. (E, F) Immunostaining of pC1^{SS2} neurons in control (E) and *dsx* knocking-down (F) males. Magenta represents nc82 signals, and green represents GFP signals. The images within the yellow dashed box and white dashed box are magnified 2× and 4×, respectively, and displayed on the right. Scale bars, 100μm. (G) Quantification of the number of pC1^{SS2} neurons in control and *dsx* knocking-down

males. n=10, 9 for control and experimental group respectively, *P < 0.05, Mann-Whitney test. Error bars correspond to SEM. (H) Quantification of the neuronal projection length shown in the 2× magnified images in (E) and (F). n=10 for each group, ****P < 0.0001, Mann-Whitney test. (I-K) Tussling time by *pC1*^{SS2} > *UAS-CsChrimson* (I) and *pC1*^{SS2} > *UAS-CsChrimson & UAS-dsx*^{M}*-RNAi* (J) males, which were quantified in (K). Red light activation with a light intensity of 0.02 mW/mm^2 for 1 minute was applied at the 2nd and 5th minutes. n=12, bars sharing the same letter are not significantly different. Friedman test for (I) and (J), Kruskal-Wallis test for (K).

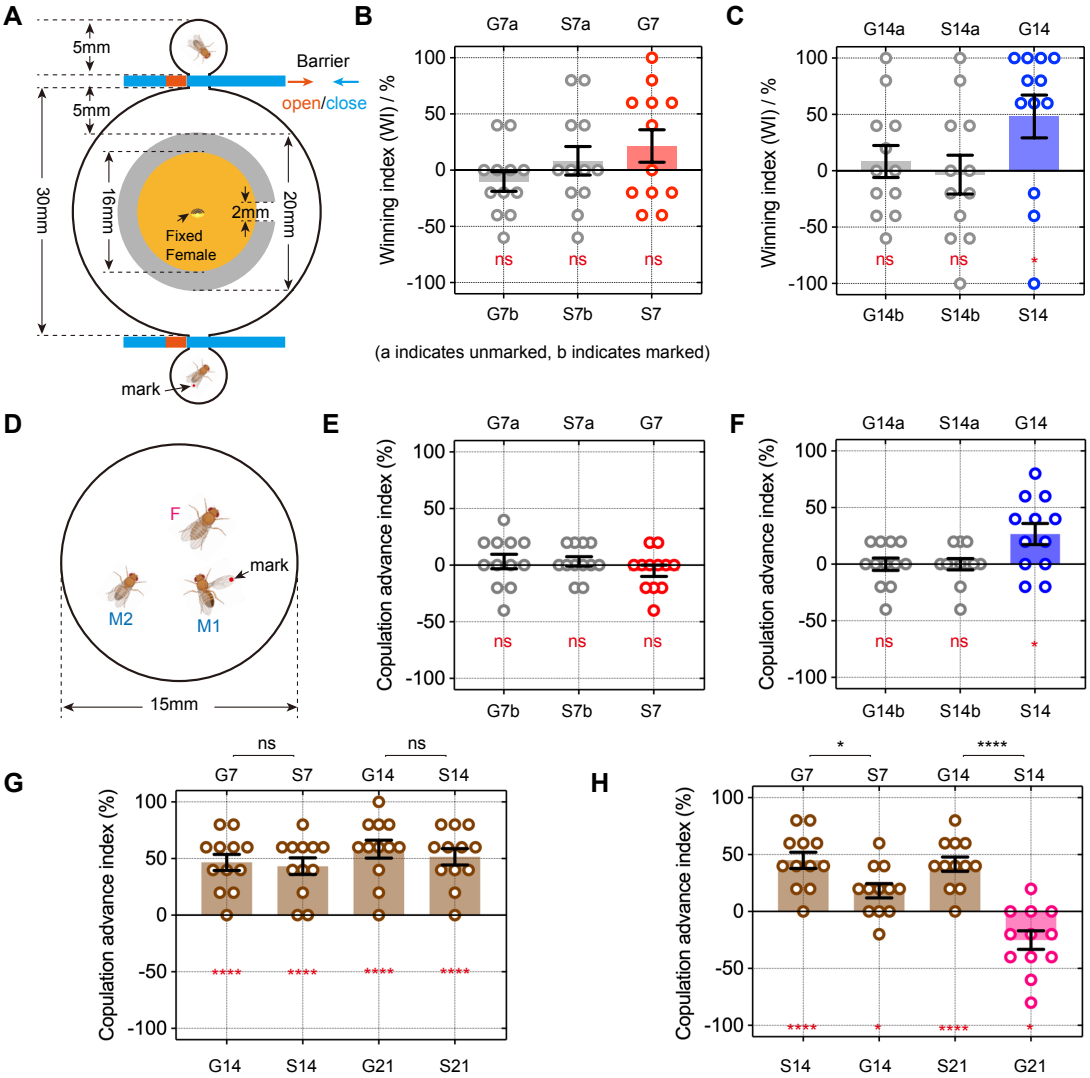

Figure 6. Social enrichment enhances male territorial control and mating competition.

(A) Schematic diagram of the paradigm for testing territorial control in males.

(B) The territorial control test of 7-day-old GH (G7) and SH (S7) males. G7a and G7b stand for marked G7 male and unmarked G7 male, respectively. n=12 for each group, n.s., not significant, one sample *t* test.

(C) The territorial control test of 14-day-old GH (G14) and SH (S14) males. n=12 for each group, n.s., not significant, *P < 0.05, one sample *t* test.
(D) Schematic diagram of the paradigm for testing male mating advantage.
(E) The mating competition test between G7 and S7 males. n=12 for each group, n.s., not significant, one sample *t* test.
(F) The mating competition test between G14 and S14 males. n=12 for each group, n.s., not significant, *P < 0.05, one sample *t* test.
(G and H) The mating competition test between young males and old males, n=12 for each group, n.s., not significant, *P < 0.05, ****P < 0.0001, one sample *t* test for comparison within group (red labeling), Mann-Whitney test for comparison between groups (black labeling). Error bars correspond to SEM.

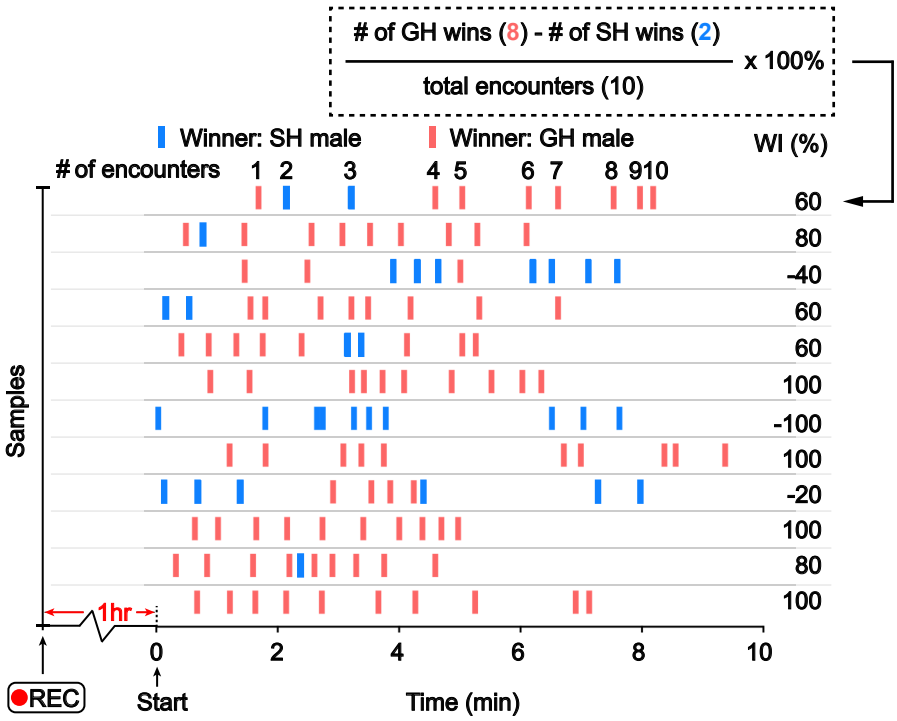

Figure 6-figure supplement 1. Winning events of representative samples for territorial competition.
The blue and red bars represent the wins for S14 males and G14 males, respectively. An example formula is provided for calculating the winning index in the dashed box.

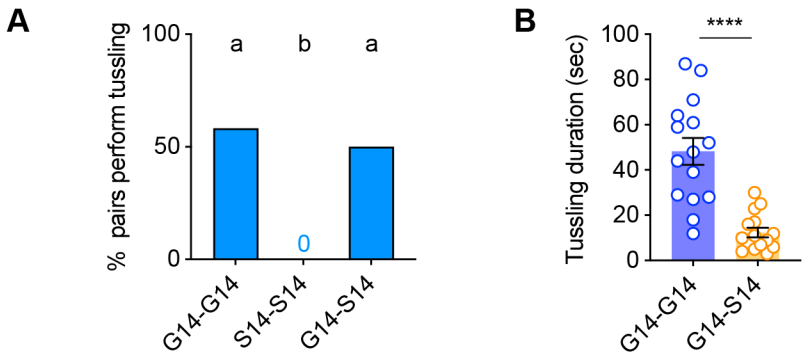

Figure 6-figure supplement 2. The occurrence and duration of tussling behavior in male flies under different pairing conditions.

(A) Proportion of male pairs performing tussling within 2 hours under three different pairing conditions in the territorial control paradigm. n=12 for each group, bars sharing the same letter are not significantly different according to Chi-square test.

(B) Duration of each tussling event in males under the G14-G14 and G14-S14 pairing conditions. n=15 events from 8-12 samples for each group, ****P < 0.0001, Mann-Whitney test. Error bars correspond to SEM.

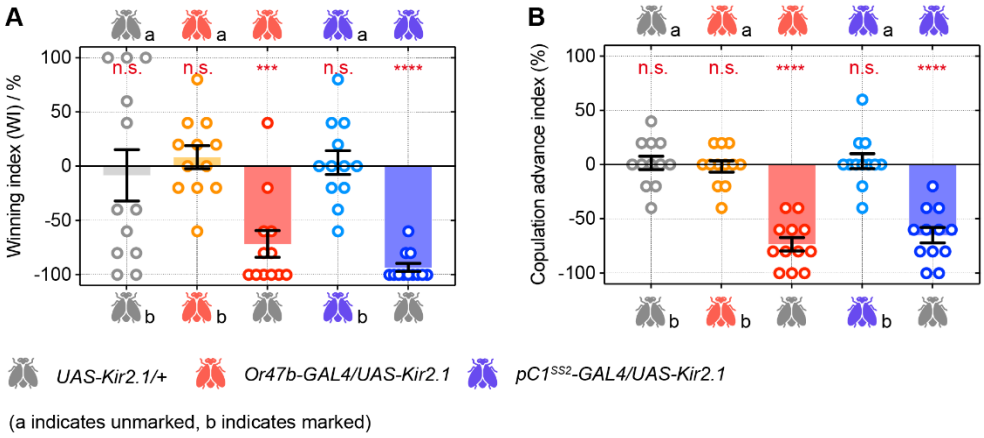

Figure 6-figure supplement 3. Silencing Or47b or pC1^{SS2} neurons compromises male territorial control and mating competition.

(A, B) Effects of Or47b neurons inactivation and pC1^{SS2} neurons inactivation on territorial control (A) and mating competition (B) in male flies. n=12 for each group, n.s., not significant, ***P < 0.001, ****P < 0.0001, one sample *t* test.

Figure 6-video supplement 1. In a territory competition paradigm, a 14-day-old group-housed (G14, marked) wild-type male consistently outcompetes a 14-day-old single-housed (S14, unmarked) wild-type male.

Figure 6-video supplement 2. In a mating competition paradigm, a 14-day-old group-housed (G14, unmarked) wild-type male outperformed a 14-day-old single-housed (S14, marked) wild-type male and successfully copulated with the female.

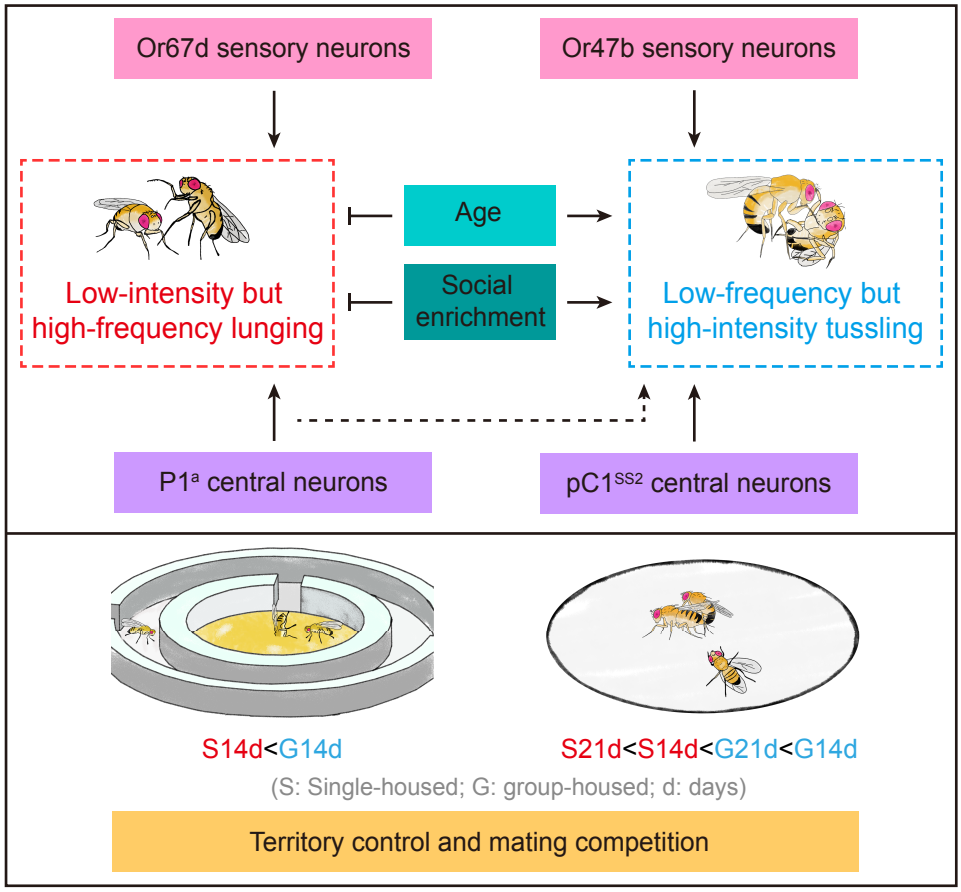

Figure 7. Summary model of fighting strategies and reproductive success in male *Drosophila*.

Age and social enrichment inhibit the low-intensity, high-frequency lunging while promoting the low-frequency, high-intensity tussling. This shift in fighting strategies among experienced, aged males can enhance their territorial control and mating competition, even offsetting aging-related mating disadvantages. Lunging and tussling behaviors are regulated by distinct sensory and central neurons.

Table S1. Detailed information for fly stocks.

Figures	Genotypes	Housing conditions	Sample sizes
Figure 1			
B	*Canton-S*	GH-2d, GH-7d, GH-14d	n=30, 30, 30, 46, 46, 46
C	*Canton-S*	GH-14d	n=30 for each group
D	*Canton-S*	GH-14d	n=30 for each group
Figure 2			
B	*Canton-S*	SH-14d, GH-14d	
C, D, E, F	*Canton-S*	SH-14d, GH-14d	n=27 for SH, n=30 for GH
G	*Canton-S*	SH-14d, GH-14d	n=30 events from 10 samples for each group
Figure 3			
A, B, C, D	*w+;;UAS-Kir2.1/+*	GH-14d	30
	w+;;Or67d-GAL4/UAS-Kir2.1	GH-14d	30
	w+;Or65a-GAL4/+;UAS-Kir2.1/+	GH-14d	30
	w+;;Or47b-GAL4/UAS-Kir2.1	GH-14d	30
	w+;;Ir84a-GAL4/UAS-Kir2.1	GH-14d	30
E, F	*w+;;Or47b-GAL4/+*	GH-14d	30
	w+;;Or47b-GAL4/UAS-Or47b-RNAi	GH-14d	30
	w+;;Or47b-GAL4/UAS-fruMi	GH-14d	30
G, H	*w+;;Or47b-GAL4/+*	GH-14d	60
	w+;;Or47b-GAL4/UAS-NaChBac	GH-14d	60
	w+;;Or47b-GAL4/+	SH-14d	60
	w+;;Or47b-GAL4/UAS-NaChBac	SH-14d	49
Figure 4			
A, B	*w+;;UAS-Kir2.1/+*	GH-14d	30
	w+;;R19B03-GAL4/UAS-Kir2.1	GH-14d	30
	w+;R15A01-AD/+;R71G01-DBD/UAS-Kir2.1 (*P1*^{a} > *UAS-Kir2.1*)	GH-14d	30
	w+;;TK-GAL4/UAS-Kir2.1 (GH-14d)	GH-14d	30
	w+;VT002064-AD/+;VT008469DBD/UAS-Kir2.1 (*pC1*^{SS1} > *UAS-Kir2.1*)	GH-14d	30
	w+;;VT002064-AD,dsxDBD/UAS-Kir2.1 (*pC1*^{SS2} > *UAS-Kir2.1*)	GH-14d	30
C	*w-;R15A01-AD/UAS-myrGFP; R71G01-DBD/+* (*P1*^{a} > *UAS-GFP*)	GH-5-7d	
D	*w-;UAS-myrGFP/+;VT002064-AD,dsxDBD/+* (*pC1*^{SS2} > *UAS-GFP*)	GH-5-7d	

F, G, H	*w-;;UAS-CsChrimson/+*	GH-5-7d	32
I, J, K	*w-;R15A01-AD/+;R71G01-DBD/ UAS-CsChrimson* (*P1*^{a} > *UAS-CsChrimson*)	GH-5-7d	32
L, M, N	*w-;;VT002064-AD,dsxDBD/UAS-CsChrimson* (*pC1*^{SS2} > *UAS-CsChrimson*)	GH-5-7d	32
Figure 5			
A, B, C, D	*w-;R15A01-AD/UAS-myrGFP; R71G01-DBD/+* (*P1*^{a} > *UAS-GFP*)	GH-5-7d	n=5 for each group (B) n=9 for each group (D)
	w-;UAS-myrGFP/+;VT002064-p65AD,dsxDBD/+ (*pC1*^{SS2} > *UAS-GFP*)	GH-5-7d	
E	*w-;UAS-CsChrimson/+;VT002064-AD, dsxDBD/+* (*pC1*^{SS2} > *UAS-CsChrimson*)	GH-5-7d	
F	*w-;UAS-CsChrimson/+; VT002064-AD, dsxDBD/UAS-dsx*^{M}*-RNAi* (*pC1*^{SS2} > *UAS-CsChrimson & UAS-dsx*^{M}*-RNAi*)	GH-5-7d	
G	*w-;UAS-CsChrimson/+;VT002064-AD, dsxDBD/+* (*pC1*^{SS2} > *UAS-CsChrimson*)	GH-5-7d	10
	w-;UAS-CsChrimson/+;VT002064-AD, dsxDBD/UAS-dsx^{M}*-RNAi* (*pC1*^{SS2} > *UAS-CsChrimson & UAS-dsx*^{M}*-RNAi*)	GH-5-7d	9
H	*w-;UAS-CsChrimson/+;VT002064-AD, dsxDBD/+* (*pC1*^{SS2} > *UAS-CsChrimson*)	GH-5-7d	10
	w-;UAS-CSChrimson/+;VT002064-AD, dsxDBD/UAS-dsx^{M}*-RNAi* (*pC1*^{SS2} > *UAS-CsChrimson & UAS-dsx*^{M}*-RNAi*)	GH-5-7d	10
I	*w-;UAS-CsChrimson/+;VT002064-AD, dsxDBD/+* (*pC1*^{SS2} > *UAS-CsChrimson*)	GH-5-7d	12
J	*w-;UAS-CsChrimson/+;VT002064-AD, dsxDBD/UAS-dsx*^{M}*-RNAi* (*pC1*^{SS2} > *UAS-CsChrimson & UAS-dsx*^{M}*-RNAi*)	GH-5-7d	12
K	*w-;UAS-CsChrimson/+;VT002064-AD, dsxDBD/+* (*pC1*^{SS2} > *UAS-CsChrimson*)	GH-5-7d	12
	w-;UAS-CsChrimson/+;VT002064-AD, dsxDBD/UAS-dsx^{M}*-RNAi* (*pC1*^{SS2} > *UAS-CsChrimson & UAS-dsx*^{M}*-RNAi*)	GH-5-7d	12

	w-;UAS-CsChrimson/+;VT002064-AD, dsxDBD/+ (*pC1^{SS2} > UAS-CsChrimson*)	GH-5-7d	12
	w-;UAS-CsChrimson/+;VT002064-AD, dsxDBD/UAS-dsx^{M}-RNAi (*pC1^{SS2} > UAS-CsChrimson & UAS-dsx^{M}-RNAi*)	GH-5-7d	12
Figure 6			
B	*Canton-S*	GH-7d	12
	Canton-S	SH-7d	12
	Canton-S	GH-7d, SH-7d	12
C	*Canton-S*	GH-14d	12
	Canton-S	SH-14d	12
	Canton-S	GH-14d, SH-14d	12
E	*Canton-S*	GH-7d	12
	Canton-S	SH-7d	12
	Canton-S	GH-7d, SH-7d	12
F	*Canton-S*	GH-14d	12
	Canton-S	SH-14d	12
	Canton-S	GH-14d, SH-14d	12
G	*Canton-S*	GH-7d, GH-14d	12
	Canton-S	SH-7d, SH-14d	12
	Canton-S	GH-14d, GH-21d	12
	Canton-S	SH-14d, SH-21d	12
H	*Canton-S*	GH-7d, SH-14d	12
	Canton-S	SH-7d, GH-14d	12
	Canton-S	GH-14d, SH-21d	12
	Canton-S	SH-14d, GH-21d	12
Figure 1-figure supplement 1			
A, B	*Canton-S*	SH-7d	12
	Canton-S	SH-14d	12
	Canton-S	GH-7d	12
	Canton-S	GH-14d	12
Figure 3-figure supplement 1			
A	*w+;;Or47b-GAL4/+*	GH-5-7d	9
	w+;;Or47b-GAL4/UAS-Or47b-RNAi	GH-5-7d	9
B	*w+;;fru^{GAL4}/+*	GH-5-7d	9

	w+;;fru^{GAL4}/UAS-fruMi	GH-5-7d	9
Figure 3-figure supplement 2			
A	*UAS-myrGFP,QUAS-mtdtomato(3xHA);trans-Tango/+;Or47b-GAL4/+*	GH-14d, 18°C	
	UAS-myrGFP,QUAS-mtdtomato(3xHA);trans-Tango/+;Or47b-GAL4/+	SH-14d, 18°C	
B	*UAS-myrGFP,QUAS-mtdtomato(3xHA);trans-Tango/+;Or47b-GAL4/+*	GH-14d, 18°C	10
	UAS-myrGFP,QUAS-mtdtomato(3xHA);trans-Tango/+;Or47b-GAL4/+	SH-14d, 18°C	8
Figure 4-figure supplement 1			
B	*w+;UAS-dTrpA1/+* (light, 22°C)	GH-5-7d	18
	w+;R15A01-AD/UAS-dTrpA1; R71G01-DBD/+ (*P1^{a} > UAS-dTrpA1*) (light, 22°C)	GH-5-7d	18
	w-;UAS-dTrpA1/+; VT002064-AD, dsxDBD/+ (*pC1^{SS2} > UAS-dTrpA1*) (light, 22°C)	GH-5-7d	18
	w+;UAS-dTrpA1/+ (dark, 22°C)	GH-5-7d	18
	w+;R15A01-AD/UAS-dTrpA1;R71G01-DBD/+ (*P1^{a} > UAS-dTrpA1*) (dark, 22°C)	GH-5-7d	18
	w-;UAS-dTrpA1/+;VT002064-AD, dsxDBD/+ (*pC1^{SS2} > UAS-dTrpA1*) (dark, 22°C)	GH-5-7d	18
	w+;UAS-dTrpA1/+ (light, 30°C)	GH-5-7d	18
	w+;R15A01-AD/UAS-dTrpA1;R71G01-DBD/+ (*P1^{a} > UAS-dTrpA1*) (light, 30°C)	GH-5-7d	18
	w-;UAS-dTrpA1/+;VT002064-AD, dsxDBD/+ (*pC1^{SS2} > UAS-dTrpA1*) (light, 30°C)	GH-5-7d	18
	w+;UAS-dTrpA1/+ (dark, 30°C)	GH-5-7d	18
	w+;R15A01-AD/UAS-dTrpA1;R71G01-DBD/+ (*P1^{a} > UAS-dTrpA1*) (dark, 30°C)	GH-5-7d	18
	w-;UAS-dTrpA1/+;VT002064-AD, dsxDBD/+ (*pC1^{SS2} > UAS-dTrpA1*) (dark, 30°C)	GH-5-7d	18
Figure 4-figure supplement 2			
retro-Tango	*QUAS-mtdTomato(3xHA);retro-Tango/R15A01-AD;UAS-EGFP/R71G01-DBD* (*P1^{a} > retro-Tango*)	GH-14-21d	

	QUAS-mtdTomato(3xHA);retro-Tango/+;UAS-EGFP/VT002064AD,dsxDBD (*pC1^{SS2} > retro-Tango*)	GH-14-21d	
GFP	*w-;R15A01-AD/+;R71G01-DBD/UAS-myrGFP* (*P1^{a} > GFP*)	GH-5-7d	
	w-;;VT002064AD,dsxDBD/UAS-myrGFP (*pC1^{SS2} > GFP*)	GH-5-7d	
trans-Tango	*UAS-myrGFP,QUAS-mtdtomato(3xHA);trans-Tango/R15A01-AD;R71G01-DBD/+* (*P1^{a} > trans-Tango*)	GH-14-21d	
	UAS-myrGFP,QUAS-mtdtomato(3xHA);trans-Tango/+;VT002064AD,dsxDBD/+ (*pC1^{SS2} > trans-Tango*)	GH-14-21d	
Figure 6-figure supplement 1			
	Canton-S	GH-14d, SH-14d	12
Figure 6-figure supplement 2			
A	*Canton-S*	GH-14d	12
	Canton-S	SH-14d	12
	Canton-S	GH-14d, SH-14d	12
B	*Canton-S*	GH-14d	n=15 events from 8-12 samples for each group
	Canton-S	GH-14d, SH-14d	n=15 events from 8-12 samples for each group
Figure 6-figure supplement 3			
A	*w+;;UAS-Kir2.1/+*	GH-14d	12
	w+;;Or47b-GAL4/UAS-Kir2.1	GH-14d	12
	w+;;Or47b-GAL4/UAS-Kir2.1 w+;;UAS-Kir2.1/+	GH-14d	12
	w+;;VT002064AD,dsxDBD/ UAS-Kir2.1(*pC1^{SS2} > UAS-Kir2.1*)	GH-14d	12
	w+;;VT002064AD, dsxDBD/ UAS-Kir2.1(*pC1^{SS2} > UAS-Kir2.1*) *w+;;UAS-Kir2.1/+*	GH-14d	12
B	*w+;;UAS-Kir2.1/+*	GH-14d	12
	w+;;Or47b-GAL4/UAS-Kir2.1	GH-14d	12
	w+;;Or47b-GAL4/UAS-Kir2.1 w+;;UAS-Kir2.1/+	GH-14d	12
	w+;;VT002064AD,dsxDBD/ UAS-Kir2.1(*pC1^{SS2} > UAS-Kir2.1*)	GH-14d	12

	w+;;VT002064AD, dsxDBD/ UAS-Kir2.1(*pC1*^{SS2} > *UAS-Kir2.1*) *w+;;UAS-Kir2.1/+*	GH-14d	12

974

975

976 **Table S2. Detailed comparison for territorial control and mating competition.**

Territorial control assay				
	pairs	**winning index**	**P value**	**conclusion**
Fig. 6B	G7a vs G7b	-10±30.15	0.275	/
	S7a vs S7b	8.33±43.87	0.524	/
	G7 vs S7	21.66±50.06	0.1619	/
Fig. 6C	G14a vs G14b	8.33±49.33	0.5702	/
	S14a vs S14b	-3.33±59.60	0.8499	/
	G14 vsS14	48.33±65.76	0.0272	G14>S14

Mating competition assay				
	pairs	**copulation advance index**	**P value**	**conclusion**
Fig. 6E	G7a vs G7b	3.33±22.29	0.6147	/
	S7a vs S7b	3.33±14.35	0.4382	/
	G7 vs S7	-5±17.32	0.3388	/
Fig. 6F	G14a vs G14b	0±19.07	>0.9999	/
	S14a vs S14b	0±17.06	>0.9999	/
	G14 vs S14	26.67±32.29	0.0155	G14>S14
Fig. 6G	G7 vs G14	46.67±24.62	<0.0001	G7>G14
	S7 vs S14	43.33±25.35	<0.0001	S7>S14
	G14 vs G21	58.33±27.58	<0.0001	G14>G21
	S14 vs S21	51.67±24.80	<0.0001	S14>S21
Fig. 6H	G7 vs S14	45±24.31	<0.0001	G7>S14
	S7 vs G14	18.33±21.67	0.0137	S7>G14
	G14 vs S21	41.67±21.67	<0.0001	G14>S21
	S14 vs G21	-25±28.44	0.0112	S14<G21
		S21<S14<G21<G14		